



Universität für Bodenkultur Wien

Department für Bautechnik und Naturgefahren

Institut für Konstruktiven Ingenieurbau

Peter-Jordanstraße 82, 1190 WIEN

Masterarbeit

Investigation of glass panel failure
of a high rise building through
monitoring based system identification

Mess- und Modelltechnische Ermittlung
von Schadensursachen an einer
Hochhausstruktur im arabischen Raum

Felix Wenzel

Wien, Mai 2015

universität des lebens

Masterarbeit zur Erlangung des akademischen Grades Diplom Ingenieur der
Studienrichtung Kulturtechnik und Wasserwirtschaft an der Universität für
Bodenkultur Wien

Betreuung:

Assoc.Prof. DI Dr. Alfred Strauss

DI Dr. Thomas Zimmermann

eingereicht von

Felix Wenzel

Matr.Nr.: 0840554

Eidesstaatliche Erklärung zur Masterarbeit

Ich versichere hiermit, diese Masterarbeit selbstständig und lediglich unter Benutzung der angegebenen Quellen verfasst zu haben.

Die vorliegende Arbeit wurde bisher noch nicht im Rahmen eines anderen Prüfungsverfahrens eingereicht.

Wien, am

.....

Felix Wenzel

Danksagung

Zunächst möchte ich mich bei all denjenigen bedanken, die mich während der Anfertigung dieser Diplomarbeit unterstützt und motiviert haben.

Ganz besonderer Dank gilt meinen Eltern die mich während des gesamten Studiums, bedingungslos unterstützt haben.

Ein herzliches Dankeschön geht an die gesamte Belegschaft der BOKU die mir unvergessliche Jahre beschert hat. Hervorheben möchte ich das IKI, das mein Interessen für's Thema geweckt hat und besonders den Herr Prof Straus der meine Diplomarbeit betreut.

Zu guter Letzt danke ich meiner Freundin die immer zu mir gehalten hat.

Kurzfassung

Durch den Bauboom des letzten Jahrzehnts sind zahlreiche Hochhäuser mit Glasfassaden in den Vereinigten Arabischen Emiraten gebaut worden. Die ungewöhnliche Häufung von Schäden an Glaselementen hat zu vertieften Untersuchungen der Ursachen und Zusammenhänge geführt.

Die Firma VCE hat den Auftrag erhalten eine Hochhausstruktur in Dubai messtechnisch zu erfassen und anschließend die Ursache des Versagens von insgesamt mehr als 25 Glaspaneelen zu identifizieren.

Dazu fanden Messungen sowohl an der Gebäudestruktur als auch an der Glasfassade statt. Ein umfangreicher Datensatz ist vorhanden.

Als Vorgangsweise wurde vorgeschlagen eine klassische Systemidentifikation auf globalem (Gesamtstruktur) als auch lokalem (Glaspaneele) Niveau durchzuführen. Detaillierte Finite-Element-Modelle, welche das theoretische Verhalten der Struktur zeigen sollen, werden erstellt. Aus der Messung sind die Parametereigenfrequenz, Eigenform und Dämpfung bekannt und können zur Systemidentifikation verwendet werden. In Korrelation mit den zu den Schadensfällen passenden Klimadaten wird ein realistisches Verhaltensmodell entwickelt, aus welchem Detailbeanspruchungen einzelner Elemente (i.e. die Glaspaneele) entnommen werden können. Es ist zu erwarten, dass die Schadensursache dadurch gefunden werden kann.

Die Arbeit bezieht sich auf einen komplexen, praktischen Anwendungsfall der Systemidentifikation und umfasst alle Schritte von der Planung des Experiments, der messtechnischen Durchführung, der Modelerstellung, der Systemidentifikation und der Ermittlung der Schadensursache.

Abstract

The purpose of this work is to find the cause for glass panel failure of a high rise building in Dubai, UAE (United Arab Emirates). This kind of damage is common for skyscrapers with glass façade elements and presents a valid danger to pedestrians. Vienna consulting engineers (VCE) was commissioned to find out if the structural behaviour or the fixing of the glass is the cause of this failure.

In order to do this VCE conducted a Structural Health Monitoring (SHM) campaign to assess the behaviour of the building and find out if the building movement can cause glass failure. Secondly the single structural member (glass element) was investigated to see if the failure has a local cause.

As a result of this monitoring campaign, classic system identification has been made. Movements and structural behaviour has been measured and evaluated based on a finite element model of the structure. As expected, after such a short lifetime, the building is in very good condition. Nonetheless the movement of the building is greater than expected which can be a cause for glass failure. Furthermore the fixing of the glass elements is very stiff which can also result in glass failure.

The evaluated causes are two of many possibilities which can lead to glass failure. As a conclusion a list of possible reasons for the investigated glass failure is given. The reaction of the building management was to build arcades and sun roofs to protect pedestrians and valuables from falling glass. Otherwise no measures have been taken.

Contents

Kurzfassung	I
Abstract	II
Contents	III
1 Introduction	1
1.1 Scope of work	1
1.2 Description of the Assessment Procedure	2
1.3 Description of the building	3
2 Modelling	6
2.1 Modelling of a high rise building.....	6
2.1.1 Elements	7
2.1.2 Boundary conditions	8
2.1.3 Loading.....	10
2.1.4 Material.....	10
2.2 Calculation of dynamic behavior	10
2.3 Modelling of glass panel	16
2.3.1 Geometry	16
2.3.2 Modelling.....	16
2.3.3 Calculation of dynamic behaviour	17
3 Monitoring	21
3.1 Framework monitoring setup for high rise building.....	21
3.1.1 Equipment.....	21
3.1.2 Layout	24
3.2 Framework monitoring setup for glass panel	26
3.2.1 Equipment.....	26
3.2.2 Layout	27
3.3 Execution of a monitoring project.....	29
3.3.1 Off-site work.....	30
3.3.2 On-site Work	31

3.3.3	Measurement	32
4	Measurement results	35
4.1	Key parameters of high rise buildings	36
4.1.1	Natural Frequencies	36
4.1.2	Mode Shapes	39
4.1.3	Vibration Intensity.....	43
4.1.4	Evaluation of Structural Integrity	44
4.2	Key parameters of the Glass Panel	46
4.2.1	Signals	46
4.2.2	Natural Frequencies	47
4.2.3	Mode Shapes	48
4.2.4	Comparison between the measured Panels.....	50
4.3	Additional investigation of the glass elements	52
4.3.1	Buckling stress of façade elements.....	52
4.3.2	Long term observations	55
5	Comparison of Measurement and Simulation.....	58
5.1	Tower Structure	58
5.2	Glass Façade Elements.....	59
6	Interpretation of Measurement Results.....	61
6.1	Potential Risks for Glass Panel Breakage at High Rise Buildings	61
6.2	Findings of the Investigation of the Gold Tower with BRIMOS®.....	62
6.2.1	Findings for the Tower Structure.....	62
6.2.2	Findings for the Curtain Wall and the Glass Panels	63
6.3	Conclusions	64
	References.....	i
	List of Figures.....	iii
	List of Tables	vii

1 Introduction

1.1 Scope of work

This Master thesis will cover a monitoring project of the company VCE in Dubai, UAE (United Arab Emirates). The applied methods and tools will be explained and a conclusion will be presented.

Glass failure is a common damage of façades of high rise buildings. A client in the UAE approached VCE because at his skyscraper, glass failure of single glass elements was occurring. Inside Vienna, VCE had two projects with similar damage occurrences but different investigation methods in terms of monitoring. The goal of this monitoring project was to find out if the glass failure of this building in the UAE was caused by bad design or construction of the building. Problems with the glass itself were not considered.

In other words: is the movement of the building to blame for the glass failure?

In general two reasons are conceivable:

1. Problems with the design and the installation of the façade elements. Restraints and temperature effects can cause the sudden breakage of single elements.
2. The structural behaviour of the tower. The tower is very slender and the core of the tower which provides the shear stiffness shows only a small cross section. The “soft” behaviour of the tower can cause big deformations of the glass façade elements.

Ambient vibration monitoring is the most suitable assessment method for this project. Any anomalies affecting structural behaviour can be detected clearly by means of operational dynamic analysis. Along with the conventional assessment the dynamic monitoring campaign by means of BRIMOS® Structural Health Monitoring supports the determination and localisation of problematic areas based on the measured vibration behaviour of the structure. In particular the analysed Dynamic Key Performance Indicators are aiming to capture global structural behaviour (addressing the high-rise building) on the one hand and local structural behaviour (addressing the interaction with individual glass façade elements) on the other hand (VCE ZT GmbH., 2014).

In addition to dynamic measurements, finite elements models of both the tower and an individual glass element were developed. The performed numerical analysis provides an enhanced insight into the structural dynamic behaviour. The calculated parameters serve as expected values based on the undamaged condition. The model is a key part of system identification. Apart from the modelling the following steps have been taken on sight.

- Short visual inspection of the situation on-site
- Vibration measurements on the tower to capture its global dynamic behavior (8 measurement levels over the full tower height + torsion measurement)
- Measurement of the stiffness between two floors (6 measurement points distributed on the 34th and 35th floor)
- Detailed vibration measurements on two façade elements (16 measurement points on each element)
- Vibration measurements on 5 more façade elements (1 measurement point on the inner glass panel and 1 on the outer glass panel)

The information for developing the FE-model and creating a measurement layout were provided by the client. As build drawings were provided for all essential parts of the building. Those drawings were more a general overview but good enough to get reasonable results.

1.2 Description of the Assessment Procedure

The following Chapter is based on Information from (VCE, 2015)

BRIMOS® Structural Health Monitoring is a technology that allows capturing and assessing load bearing behavior of engineering structures based on the principles of structural mechanics. The monitoring technique was developed in order to be applied with a minimum of traffic impediment or operational disturbance. The measurements are always conducted under ambient (environmentally excited vibrations) condition on the one hand and under typical operational loading conditions on the other hand. The latter usually represents the most significant impact to be analyzed with regard to the structural performance.

BRIMOS® represents a well-defined assessment procedure based on the following measured dynamic parameters: Eigenfrequencies, Mode Shapes, Damping patterns along the structure, Vibration Intensity and the Trend of Structural Integrity along the structure and over time.

In addition an accompanying visual inspection focusing on obvious damage is incorporated into the evaluation. Extensive Finite Element analysis provides decisive modal parameters on the one hand and enables a deeper understanding, quantification and interpretation of the observed phenomena on the other hand.

Furthermore the results are compared to reference data from the BRIMOS® Database. The experience of about 1000 investigated structures worldwide has been incorporated into the assessment procedure (VCE, 2015).

1.3 Description of the building

The following description has been extracted and summarized from (Baytur, 2014)

For confidentiality reasons the name or address of the tower shall not be named.

The tower is 157 m high and was completed by June 2009 after a building time of about 4,5 years. The AU Tower stands tall among more than 80 towers in a Tower project.

The Tower is a state of the art office development (primary load being structure made of concrete) extending to 48.000m² consisting of a 37 story rectangular tower (plan view 50m x 33m) with curvilinear facades in gold colored curtain walling. Construction follows the shell and core approach for tenant areas while public areas and landlord areas are fully fitted out and finished. There is a one level basement containing car parking and plant / equipment and storage rooms while the ground floor is dedicated to retail and food outlets.

The figures below show the 35th floor plan (Figure 1) and the ground floor plan (Figure 2) of the building. Figure 3 shows the tower and façade. Figure 4 shows a floor plain without interior finish.

General Information:

- Total Approx. Closed Area = 48,000 m²
- Total Number of Office Story: 37 Floors
- Location of Project: Dubai, UAE
- Total Amount of Structural Concrete: Approx. 21.250m³
- Total Amount of Reinforcing Steel: Approx. 3,000 tones
- Starting Date: 25 December 2005
- Completion Date : 30 June 2009

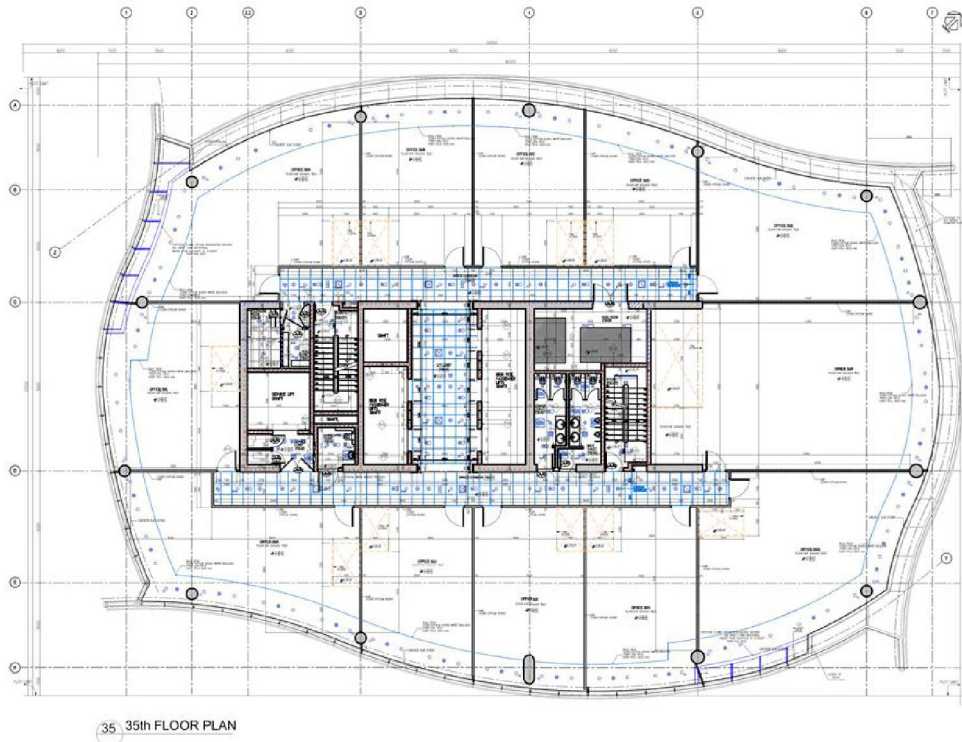


Figure 1: 35th floor plan of the building (KEO Int. & WS, 2009)

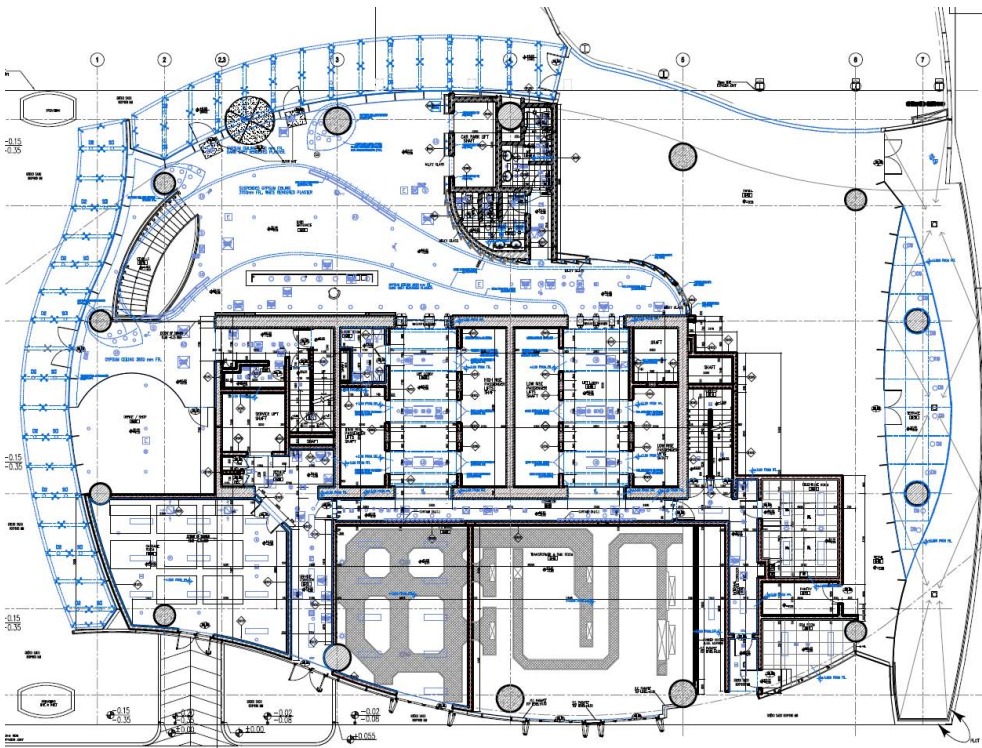


Figure 2: Ground floor plan of the building (KEO Int. & WS, 2009)



Figure 3: Photo documentation of the tower - overview



Figure 4: Photo documentation of the Tower – 37th floor

2 Modelling

For Modelling of the high rise building the commercial finite element code ANSYS (SAS IP) was used. The model of the glass panels were built with RFEM 5 with additional use of the dynamic toolbox and the buckling of steel toolbox.

2.1 Modelling of a high rise building

First Step of modelling of a high rise building is, to define the geometry. For this task the provided drawings from the client where used. There is always uncertainty in this step because of the nature of the plan, not being an as built plan.



Figure 5: Overview of the model

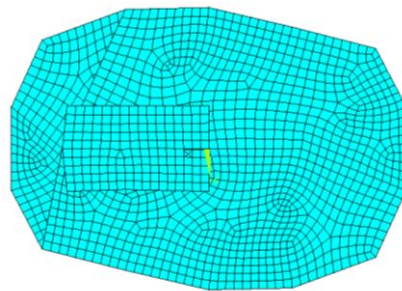


Figure 6: Crosssection of the model

2.1.1 Elements

The Element used for modelling the Columns was BEAM 44. The walls of the core were idealized as columns and also modelled with Beam 44. The slaps were modelled with SHELL 63 elements.

BEAM 44 element description

BEAM44 is a uniaxial element with tension, compression, torsion, and bending capabilities. The element has six degrees of freedom at each node: translations in the nodal x, y, and z directions and rotations about the nodal x, y, and z-axes. This element allows a different unsymmetrical geometry at each end and permits the end nodes to be offset from the centroid axis of the beam. The element is located by a reference coordinate system (x', y', z') and offsets. The reference system is defined by nodes I, J, and K, or an orientation angle. (ANSYS, 2012)

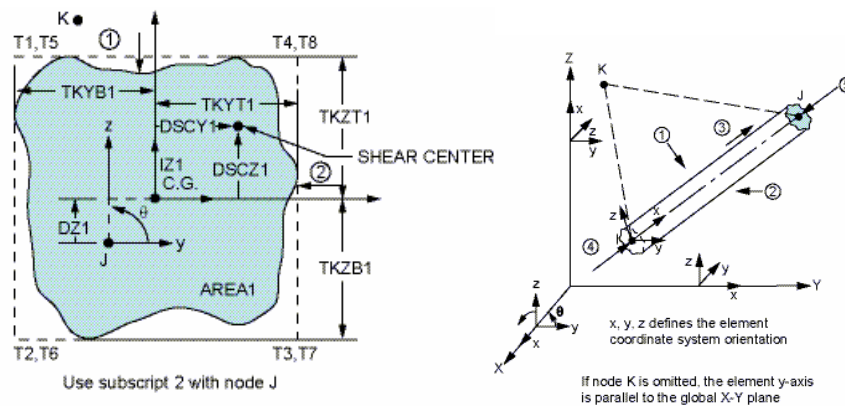


Figure 7: Beam 44 element specifics (ANSYS, 2012)

SHELL63 element description

SHELL63 has both bending and membrane capabilities. Both in-plane and normal loads are permitted. The element has six degrees of freedom at each node: translations in the nodal x, y, and z directions and rotations about the nodal x, y, and z-axes. Stress stiffening and large deflection capabilities are included. A consistent tangent stiffness matrix option is available for use in large deflection (finite rotation) analyses (ANSYS, 2012)

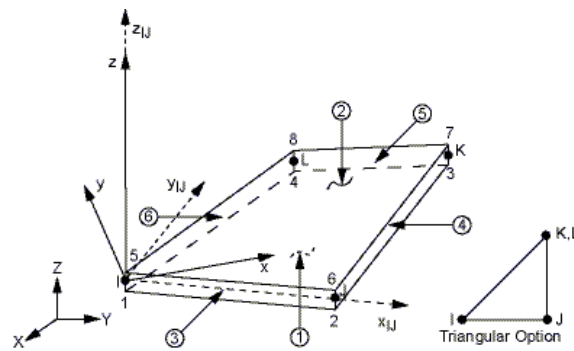


Figure 8: SHELL 63 element specifics (ANSYS, 2012)

2.1.2 Boundary conditions

The connection between the columns and walls with the slaps is assumed rigid.

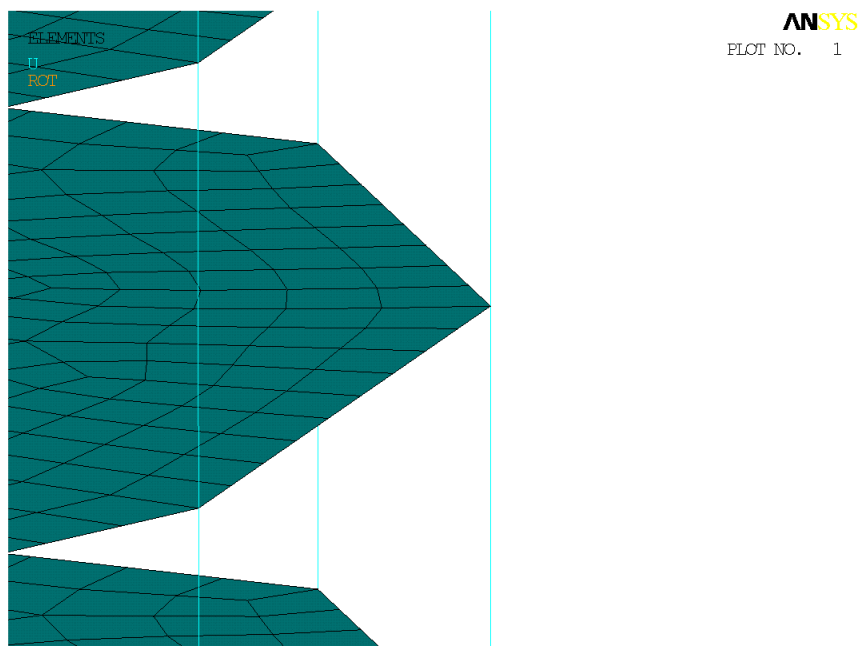


Figure 9: Connection between slab and column

The foundation of the building is modelled by longitudinal springs with 6 degrees of freedom. Those springs were applied to every column and shear wall.

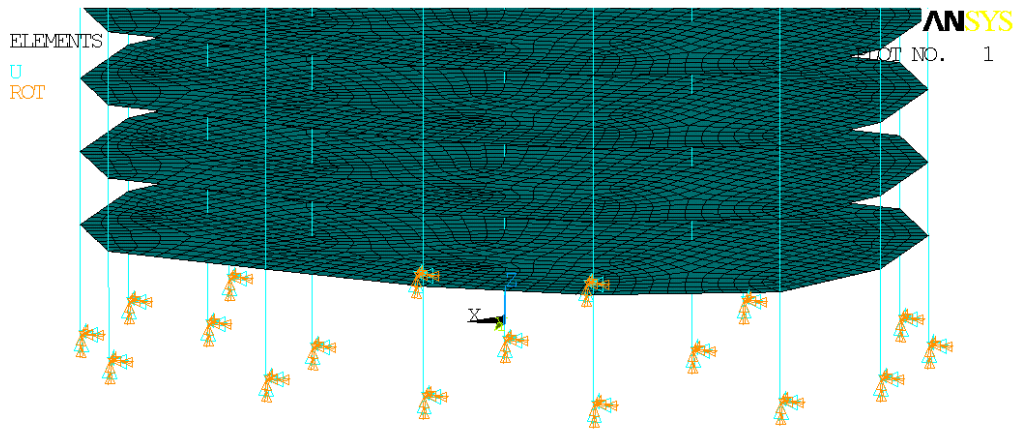


Figure 10: Foundation

Since there were no information regarding the soil or foundation stiffness, the spring stiffness was assumed with $2,7 \cdot 10^9 \text{N/m}$ for the longitudinal springs and with $2,7 \cdot 10^9 \text{ Nm}/\Phi$ for the rotational resistance.

COMBIN14 element description

COMBIN14 has longitudinal or torsional capability in 1-D, 2-D, or 3-D applications. The longitudinal spring-damper option is a uniaxial tension-compression element with up to three degrees of freedom at each node: translations in the nodal x, y, and z directions. No bending or torsion is considered. The torsional spring-damper option is a purely rotational element with three degrees of freedom at each node: rotations about the nodal x, y, and z axes. No bending or axial loads are considered. (ANSYS, 2012)

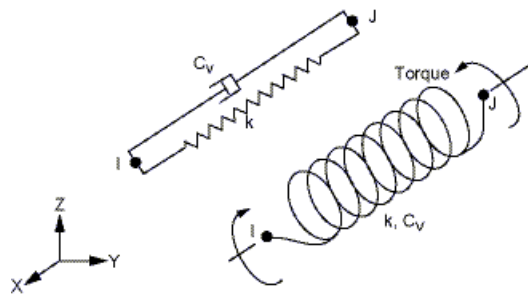


Figure 11: COBIN14 element specifics (ANSYS, 2012)

2.1.3 Loading

Permanent loading was assumed with additional 100kg/m² representing floor construction, building equipment and appliances.

Altogether, in each floor were 46 glass elements with about 100kg each. That results in 9,2 tons per floor. This additional load was modeled with MASS 21 elements. These elements were placed in each floor at the edge of the slab.

MASS21-Element description

MASS21 is a point element having up to six degrees of freedom: translations in the nodal x, y, and z directions are used in this model. The mass element is defined by a single node and concentrated mass components (Force*Time²/Length) in the element coordinate directions. (ANSYS, 2012)

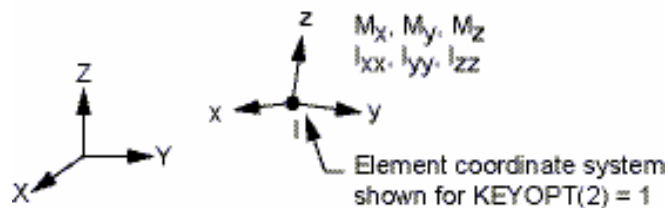


Figure 12: MASS21 element specifics (ANSYS, 2012)

2.1.4 Material

There was no specific information on the grade of the concrete so a C40/50 was assumed. This conforms the required strength for the core of such a building.

Material	E-Modulus [N/mm ²]	Poisson [-]	Density [kg/m ³]
Concrete C40/50	35000	0,2	2500

2.2 Calculation of dynamic behavior

The calculated parameters represent the expected system behavior presuming the assumed system variables correspond with reality. The calculation shows the undamaged condition of the building.

The comparison between measured and calculated behavior directly addresses structural resistance (bending/torsional resistance) in absolute values which enables to analyze probable structural deficiencies. (Znidaric, 2010)

The following table (Table 1) includes all analytically computed Eigenfrequencies for Gold Tower, which have been considered to be relevant for further evaluation. They are specified with regard to the character of motion and the origin of stressing. The corresponding mode shapes are represented from Figure 14 to Figure 21 (VCE ZT GmbH., 2014)

No.	Vibration mode (Kind of loading)	Updated FE-Model [Hz]	Spezification regard. Character of Motion and Origin of Stressing
1	1 st bending mode	0,27	1BT - 1 st bending along transversal axis
2	2 nd bending mode	0,39	1BT - 1 st bending along longitudinal axis
3	1 st torsional mode	0,67	1TL - 1 st torsion
4	3 rd bending mode	1,23	2BT - 2 nd bending along transversal axis
5	2 nd torsional mode	1,72	2TL - 2 nd torsion
6	4 th bending mode	1,65	2BT - 2 nd bending along longitudinal axis
7	5 th bending mode	2,76	3BT - 3 rd bending along transversal axis
8	6 th bending mode	3,28	3BT - 3 rd bending along longitudinal axis

Table 1: Relevant eigenfrequencies

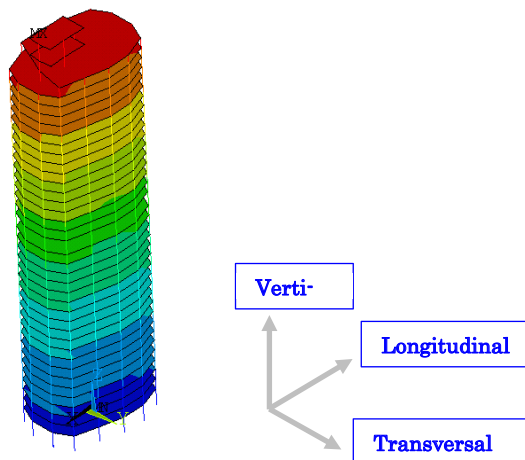
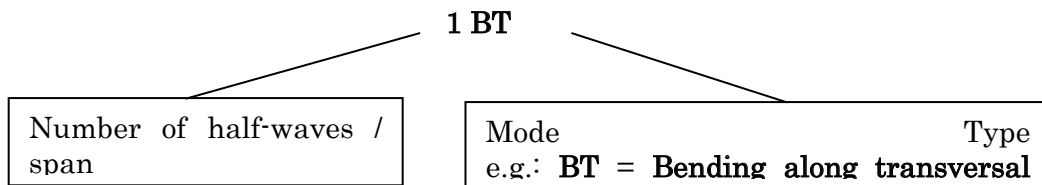


Figure 13: BRIMOS nomenclature of dynamic-response-characteristic

Figure 13 explains how the three-character BRIMOS® nomenclature - stated in the last column – is to be understood. Character one indicates the number of half cycles of the described mode shape. Character two exhibits the type of occurring mechanical motion. Character 3 assigns the associating rotation or translation axis belonging to the reference coordinate system. (VCE ZT GmbH., 2014)

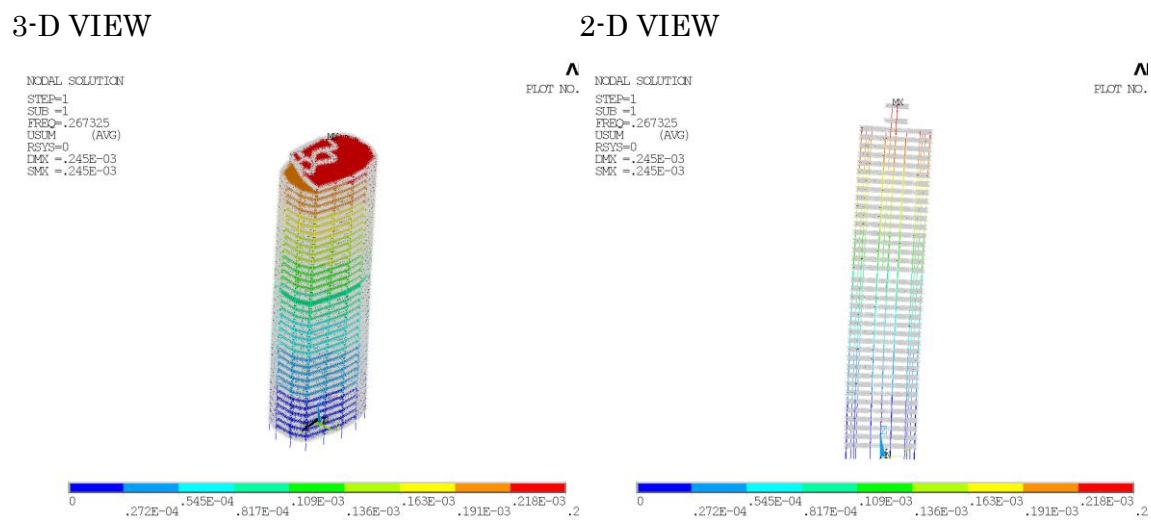


Figure 14: 1st mode shape at 0,27 Hz (numerical simulation) – 1st bending mode along transversal axis

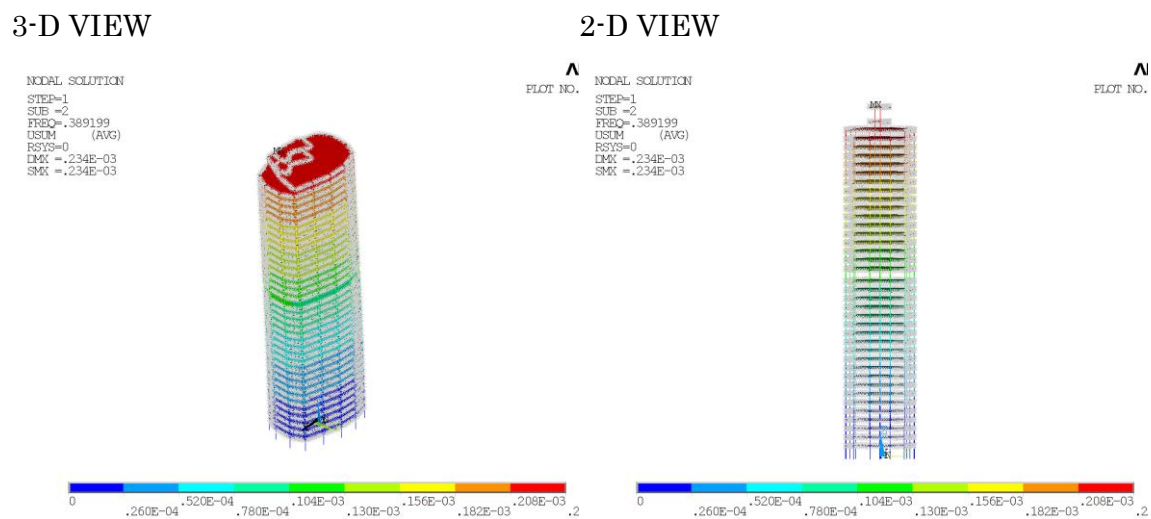


Figure 15: 2nd mode shape 0,39 Hz (numerical simulation) – 1st bending mode along longitudinal axis

3-D VIEW

NODAL SOLUTION
 STEP=1
 SUE =3
 FREQ=.667261
 USUM (AVG)
 RSYS=0
 LMX =.318E-03
 SMX =.318E-03



2-D VIEW

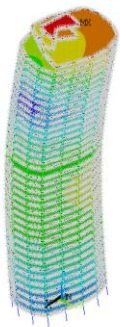
^
 PLOT NO. NODAL SOLUTION
 STEP=1
 SUE =3
 FREQ=.667261
 USUM (AVG)
 RSYS=0
 LMX =.318E-03
 SMX =.318E-03



Figure 16: 3rd mode shape – 0,67 Hz (numeric simulation) – 1st torsional mode

3-D VIEW

NODAL SOLUTION
 STEP=1
 SUE =4
 FREQ=1.225
 USUM (AVG)
 RSYS=0
 LMX =.277E-03
 SMX =.277E-03



2-D VIEW

^
 PLOT NO. NODAL SOLUTION
 STEP=1
 SUE =4
 FREQ=1.225
 USUM (AVG)
 RSYS=0
 LMX =.277E-03
 SMX =.277E-03



Figure 17: 4th mode shape – 1,23 Hz (numerical simulation) – 2nd bending mode along transversal axis

3-D VIEW

NODAL SOLUTION
 STEP=1
 SUE =5
 FREQ=1.648
 USUM (AVG)
 RSYS=0
 LMX =.240E-03
 SMX =.240E-03



2-D VIEW

^
 PLOT NO. NODAL SOLUTION
 STEP=1
 SUE =5
 FREQ=1.648
 USUM (AVG)
 RSYS=0
 LMX =.240E-03
 SMX =.240E-03



^
 PLOT NO.



Figure 18: 5th mode shape – 1,65 Hz (numerical simulation) - 2nd bending mode along longitudinal axis

3-D VIEW

NODAL SOLUTION
 STEP=1
 SUE =6
 FREQ=1.717
 USUM (AVG)
 RSYS=0
 LMX =.320E-03
 SMX =.320E-03



2-D VIEW

^
 PLOT NO. NODAL SOLUTION
 STEP=1
 SUE =6
 FREQ=1.717
 USUM (AVG)
 RSYS=0
 LMX =.320E-03
 SMX =.320E-03



^
 PLOT NO.



Figure 19: 6th mode shape – 1,72 Hz (numerical simulation) – 2nd torsional mode

3-D VIEW

NODAL SOLUTION
 STEP=1
 SUE =8
 FREQ=2.764
 USUM (AVG)
 RSYS=0
 LMX =.285E-03
 SMX =.285E-03



2-D VIEW

^
 PLOT NO. NODAL SOLUTION
 STEP=1
 SUE =8
 FREQ=2.764
 USUM (AVG)
 RSYS=0
 LMX =.285E-03
 SMX =.285E-03



Figure 20: 7th mode shape – 2,76 Hz (numerical simulation) – 3rd bending mode along transversal axis

3-D VIEW

NODAL SOLUTION
 STEP=1
 SUE =10
 FREQ=3.28
 USUM (AVG)
 RSYS=0
 LMX =.273E-03
 SMX =.273E-03



2-D VIEW

^
 PLOT NO. NODAL SOLUTION
 STEP=1
 SUE =10
 FREQ=3.28
 USUM (AVG)
 RSYS=0
 LMX =.273E-03
 SMX =.273E-03



Figure 21: 7th mode shape – 3,28 Hz (numerical simulation) – 3rd bending mode along longitudinal axis

2.3 Modelling of glass panel

2.3.1 Geometry

Two different Glass panel were modelled and later measured. One near to the ground floor witch has the same properties as the panels in the vulnerable regions and 4 panels on the 37th floor due to easy accessibility. The geometry of the glass panels were taken from the provided drawings and later checked on site. Based on that, a numerical FE-Model with the commercial finite element software RFEM was built.

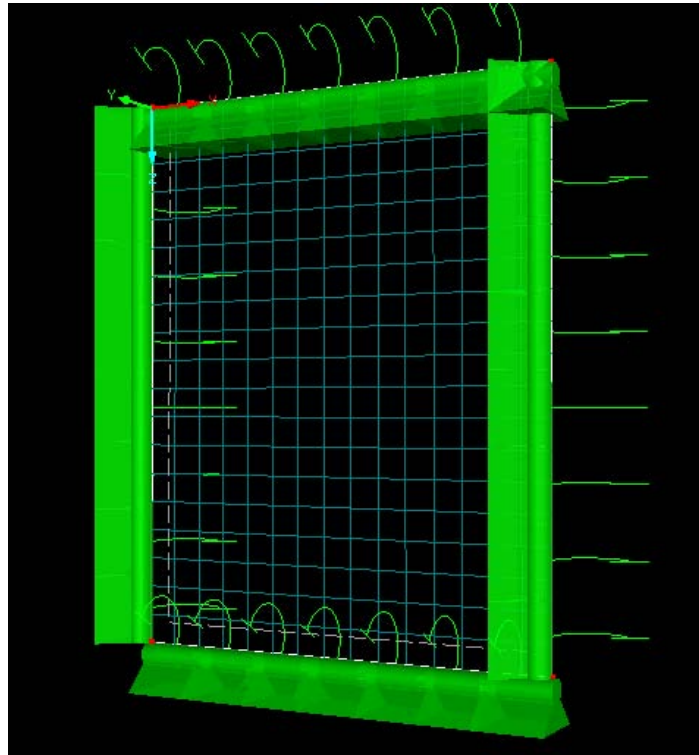


Figure 22: 3D view of the model

2.3.2 Modelling

Two selected glass elements were modelled with 2D plane elements. While the first 3 degrees of freedom were permitted (displacement) rotation springs at the planes edge were implemented.

Material	E-Modulus [KN/cm ²]	Poisson [-]	Density [kN/m ³]
Tinted Tempered Glass	7000	0,23	25

2.3.3 Calculation of dynamic behaviour

Again the calculated parameters from the numerical model represent expected values based on an initial undamaged condition. The comparison between measured and calculated behavior directly addresses structural bending resistance in absolute values which enables to analyze probable structural deficiencies (VCE ZT GmbH., 2014).

The following tables include all analytically computed eigenfrequencies for the investigated glass panels, which have been considered to be relevant for further evaluation. They are specified with regard to the character of motion and the origin of stressing. The corresponding mode shapes are represented in Figure 23 and Figure 24 (VCE ZT-GmbH., 2005).

No.	Vibration mode (Kind of loading)	FE-Model [Hz]	Spezifikation regard. Character of Motion and Origin of Stressing
1	1 st bending mode	20,40	1BT - 1 st bending around local transversal axis
2	2 nd bending mode	35,50	2BT - 2 nd bending around local transversal axis

Table 2: Relevant eigenfrequencies – single glass panel 37th floor

No.	Vibration mode (Kind of loading)	FE-Model [Hz]	Spezifikation regard. Character of Motion and Origin of Stressing
1	1 st bending mode	20,67	1BT - 1 st bending around local transversal axis
2	2 nd bending mode	37,68	2BT - 2 nd bending around local transversal axis

Table 3: Relevant eigenfrequencies – single glass panel ground floor

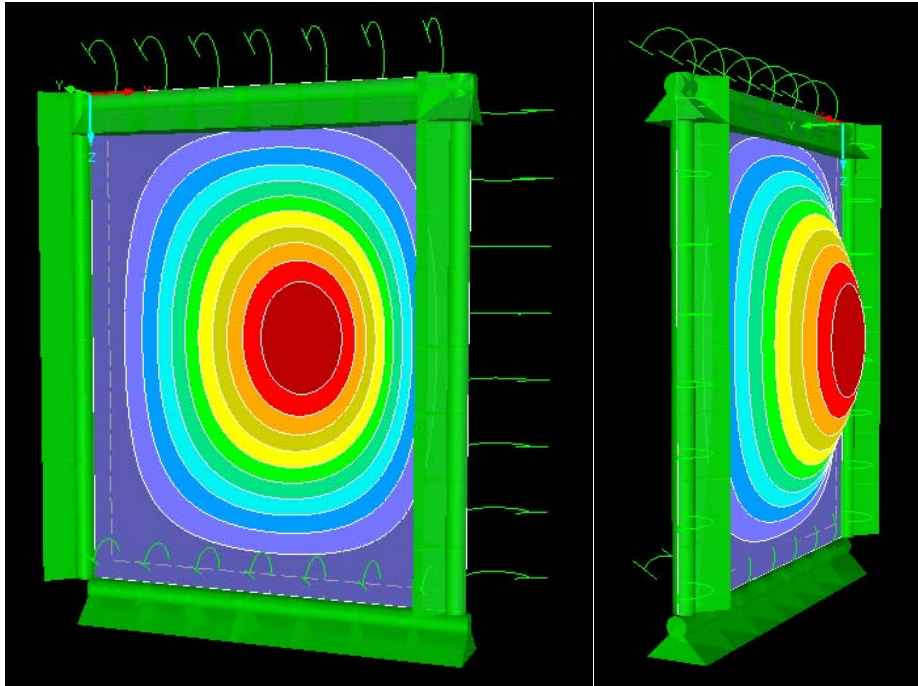


Figure 23: 1st mode shape (numerical simulation) – 1st bending around the local transversal axis

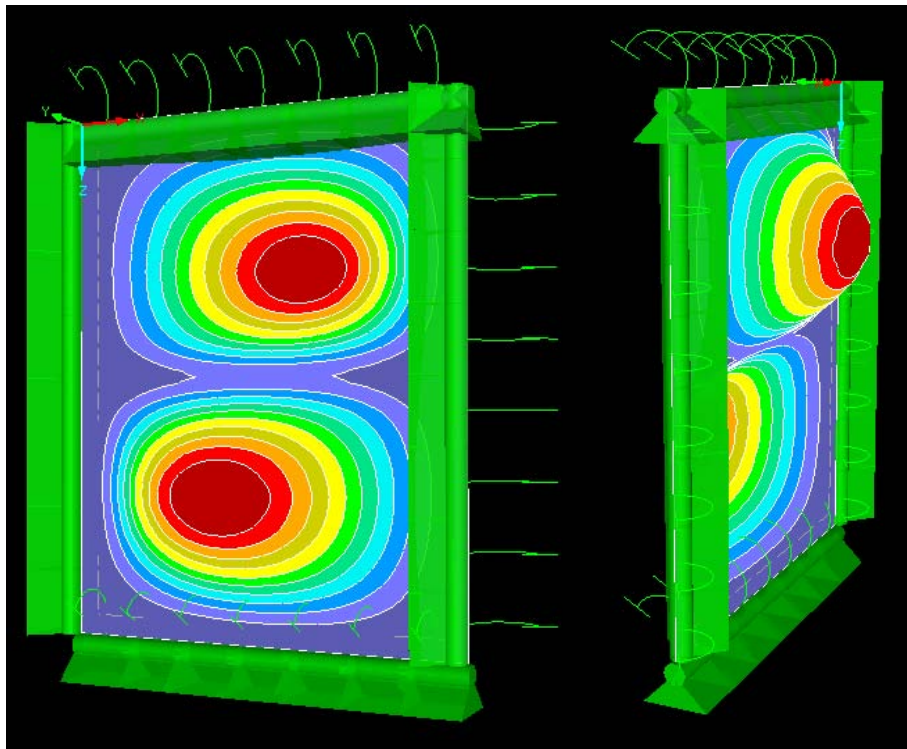


Figure 24: 2nd mode shape (numerical simulation) – 2nd bending around the local transversal axis

The following two models have been made during model updating. It shall be explained why those models were discarded as not representing reality.

The first model has no fixing of the side edges. This kind of fixing occurs when two glass elements are connected via thick elastic glue.

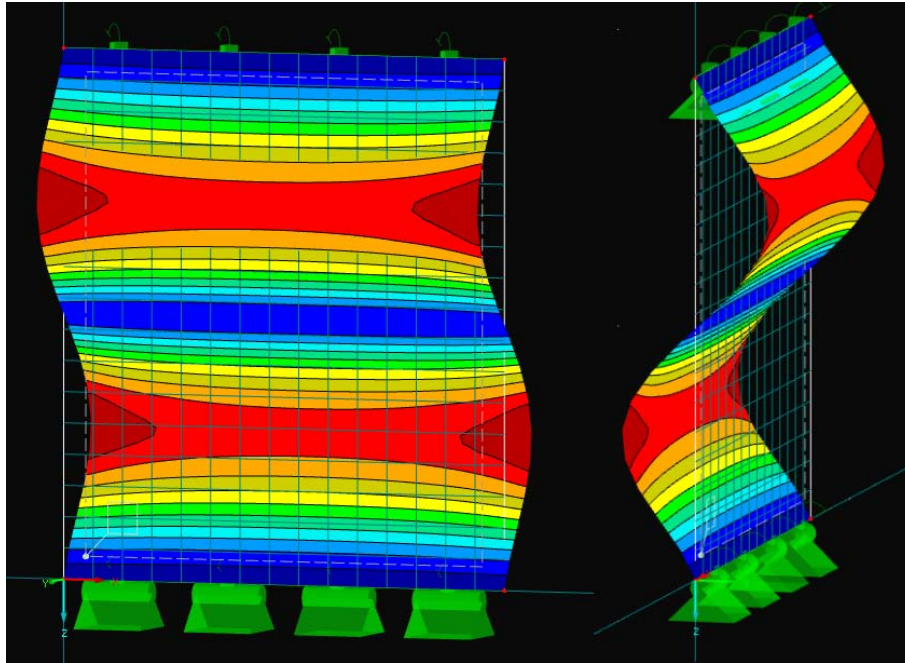


Figure 25: 4th mode shape (numerical simulation) – 2nd bending around the local transversal axis

It is easy to see that this simulation does not correlate to the measurement (seen in 4.2.3) therefore has to be discarded. The second bending mode shape occurs at the 4th eigenfrequency and additionally the frequency is much lower than the measured one ($28\text{Hz} < 38\text{Hz}$).

The second model shows the glass behaviour when the very stiff fixing (rotational sprigs) is only attached to the top and bottom edge of the glass element. Again representing a kind of fixing where the element is loosely fixed to its neighbour.

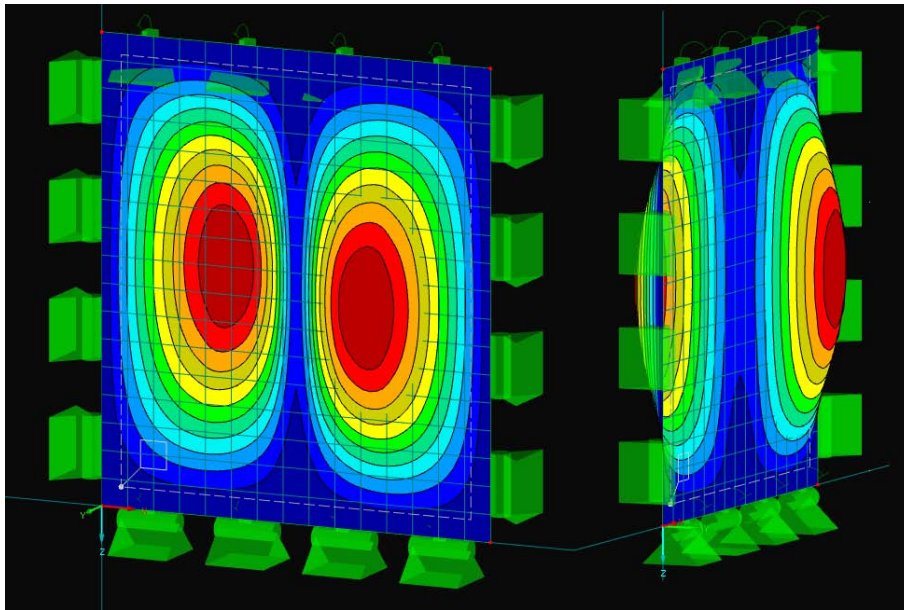


Figure 26: 2nd mode shape (numerical simulation) – 2nd bending around longitudinal axis

Later on it is easy to see that this, modelled second bending, does not correlate with the measurement (seen in 4.2.3) and therefore the model is discarded. The loosening of the side edges changed the eigenfrequency of the 2nd bending around transversal axis to the 3rd eigenfrequency.

The actual model update happens after the measurement because the measured information is needed to improve the model to be more realistic. Still it was mentioned in this chapter to keep all modelling tasks together.

3 Monitoring

The aim of this chapter is, to give a quick overview of the monitoring methods used in the surveyed building. This will be done by creating an instruction manual for monitoring a high rise building and a glass panel. These manuals should enable anyone, with the right equipment at hand, to do a structural health monitoring of any high rise building and to measure the dynamic properties of glass panels. How to process the obtained data and how to compute any result will be discussed in a later chapter.

3.1 Framework monitoring setup for high rise building

This subchapter is divided into two parts, the “equipment” part and the “Layout” part. The Equipment part describes the necessary equipment which is needed to make a dynamic assessment (structural health monitoring) of a high rise building. The Layout part shows how to place the equipment inside the building to get the best results. The Layout depends on what exactly is measured and what is investigated. The Layout introduced here is used for general structural health monitoring of the entire building.

3.1.1 Equipment

The used equipment consists of two substantial parts, sensors and data acquisition units (called sensor units SU).

Sensors

A sensor is a device whose purpose is to sense (to detect) its environment. It detects events or changes of certain surroundings and provides a corresponding output (Grimes, Dickey, & Pishko, 2006).

The used sensors are, without exception, accelerometers. An accelerometer measures the change of velocity at a certain point in time and space. Although it measures gravity it doesn't measure relative movement like the earth rotation. Because it measures gravity it can also be used to measure inclination. This is often done by VCE but not in this case.

Data acquisition unit (Sensor unit SU)

The main purpose of a data acquisition unit is to transform the, mostly analogue, measurement signal into a digital signal that can be processed by PC. The second important task is to either save the data on a local storage or to transfer it right away to the next PC.

In the gold tower project VCE used the BRIMOS Wireless system. This system consists of a 24Bit analogue to digital converter and a signal processing device. The sample rate is adjustable to a high value of 1000Hz. Data transfer is conducted with wireless LAN connection.

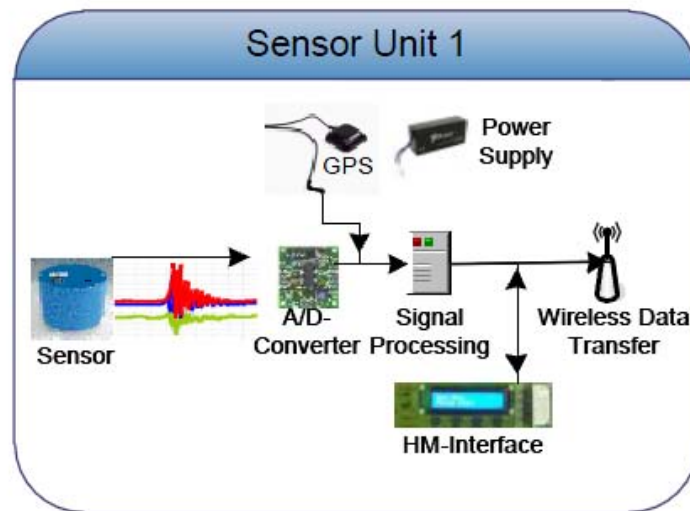


Figure 28: Flow chart of BRIMOS Wireless system (VCE, 2015)

For starting the unit GPS reception is necessary. The unit tags the recorded data with a GPS timestamp to synchronise data from different SU. This timestamp allows a synchronicity of 10 μ s between the units. Every SU has 9 channels where a signal can be applied. To measure acceleration, one channel is required for every special direction, which means a three dimensional accelerometer needs 3 channels for proper function. For more information find the datasheet in the appendix.

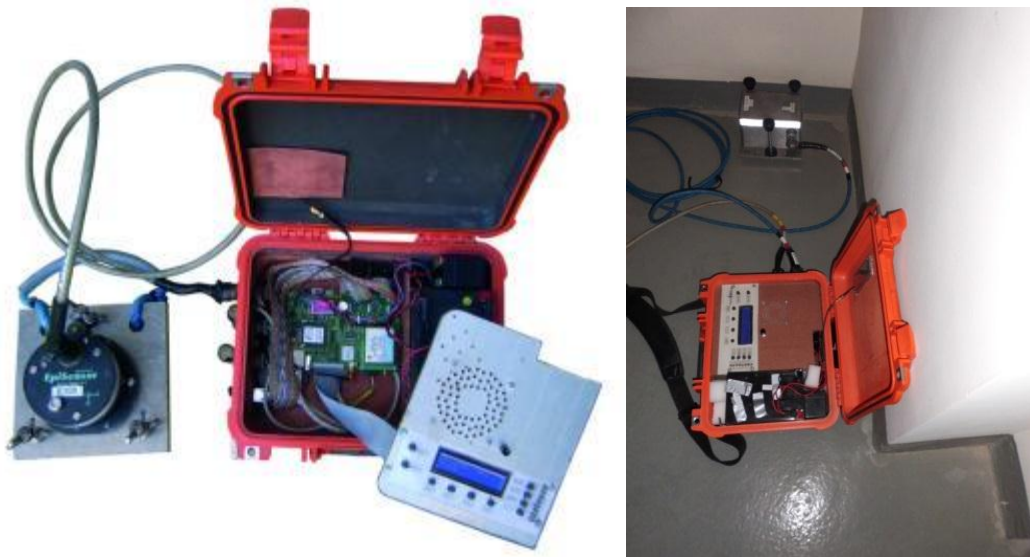


Figure 29: BRIMOS Wireless unit 1.0 plus EPI sensor example picture (left); picture taken in the gold tower (right)

3.1.2 Layout

The Layout of the measurement depends on the type of the building and the movements of the building which are especially interesting for the task at hand. In case of a global dynamic behaviour measurement of a high rise building the expected significant mode shapes consist of transversal bending and torsion. To measure the transversal bending movement, the sensors should be distributed over the height of the building and to measure the torsion the sensors should be distributed in one story preferably far from the core of the building. A reference sensor is very important for the consolidation of the data. The reference sensor should always be placed where there is the most movement considering the mode shapes. In case of a high rise building that place is the top. Eight monitoring points were distributed over the full height of the building (Floor 35, 34, 30, 26, 22, 18, 14 and 10). To achieve this goal 5 accelerometers and two BRIMOS Wireless sensor units were used.

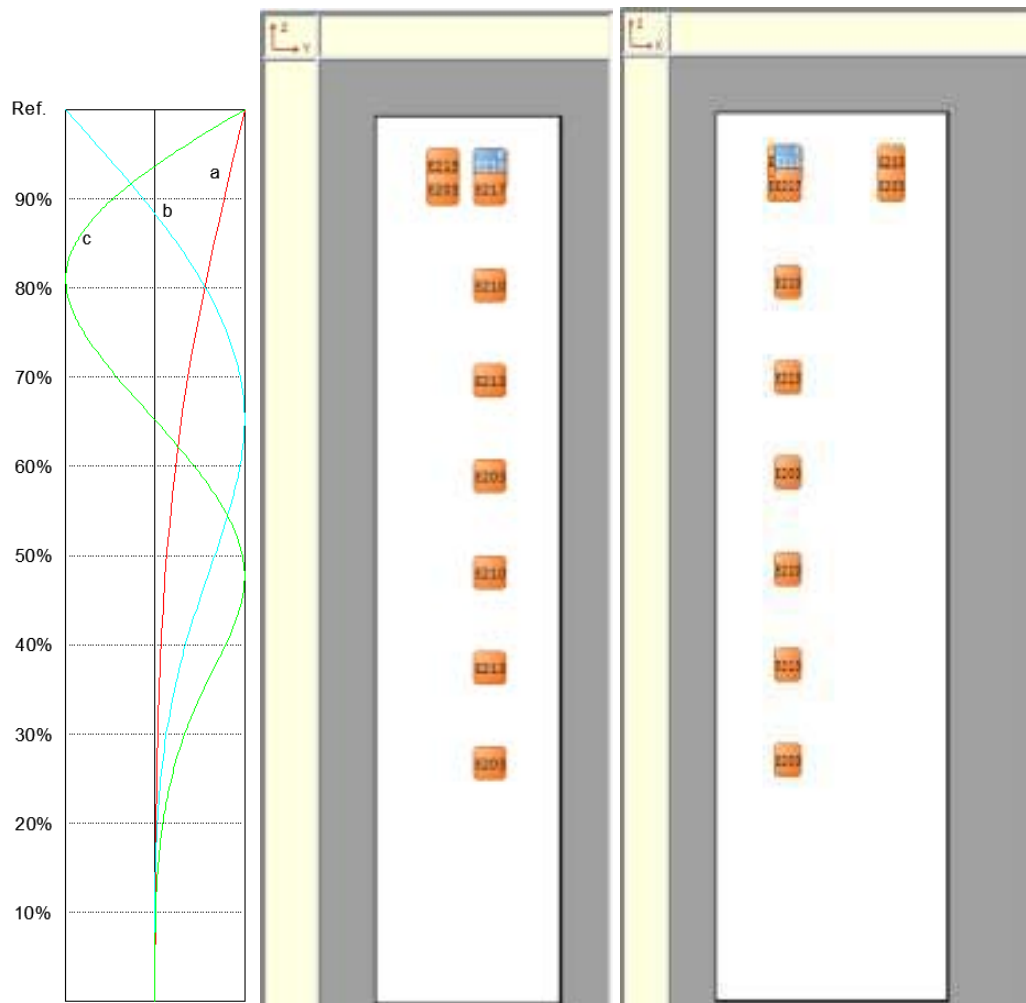


Figure 30: Sensor layout transversal movement (left): expected mode shapes. a = first Eigen frequency b = second c = third; (middle): 2d sensor layout view southwest elevation; (right): 2d sensor layout view southeast elevation

To measure the torsion the sensors have been distributed in a triangle in the upper stories. In order to measure all structural parameters that can cause the breakage of glass panels the shear stiffness between two floors was also measured. To accomplish that, six measurement points were distributed between two floors (34th and 35th floor) this also improves the accuracy of the torsion measurement.

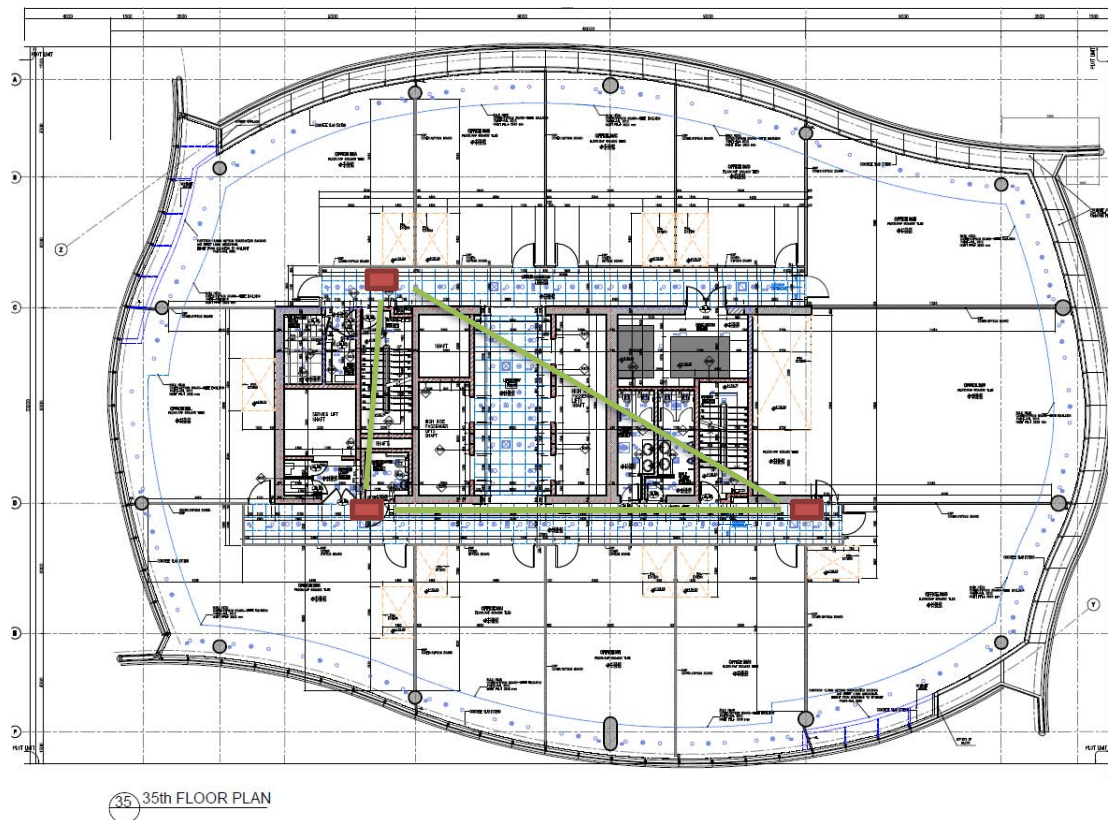


Figure 31: 35th floor plan sensor locations

3.2 Framework monitoring setup for glass panel

This subchapter describes how to measure the dynamic properties of glass panels.

3.2.1 Equipment

The equipment used is similar to above just instead of one 3D EPI sensor there are three 1D Wilcoxon sensors connected to one port of the SU.

Sensors

Because of the small weight and size of the panels (compared to the building) the Eigen frequencies are much higher. The sensors used to measure the dynamic properties of the building are not suitable for measuring such high frequencies and furthermore they are too heavy. A sensor of such weight would, attached to a

glass panel, disturb the dynamic behaviour so no accurate results can be computed.

For this purpose VCE used WILCOXON Model 731-207 Ultra low frequency seismic accelerometer. Its light weight and sensitivity for low frequencies make this sensor very well suited for this kind of measurement. For more details on the sensor find the datasheet in the appendix. The sensor is attached to the glass surface with two component epoxy resin glue.



Figure 32: Wilcoxon Model 731-207 (right); Mounting of sensor on glass surface inside and outside (left)

Data acquisition unit (Sensor unit SU)

The BRIMOS Wireless System was used (same as above). It is important to mention that the small Wilcoxon sensors need additional signal amplifier in order to produce a useable signal. These amplifiers need an external power source, in this case batteries.

3.2.2 Layout

The Layout of the sensors follows similar rules as with buildings. First the significant mode shapes with the associated Eigen frequencies has to be specified and a reference sensor has to be placed in a spot with significant movement. In case of a general dynamic assessment of the glass the reference sensor is placed in the 40% point. This point is located at 40% of the length of the object because

at this location the 1st, 2nd, 3rd and 4th Eigen frequency is measurable and the boundary conditions have less influence.

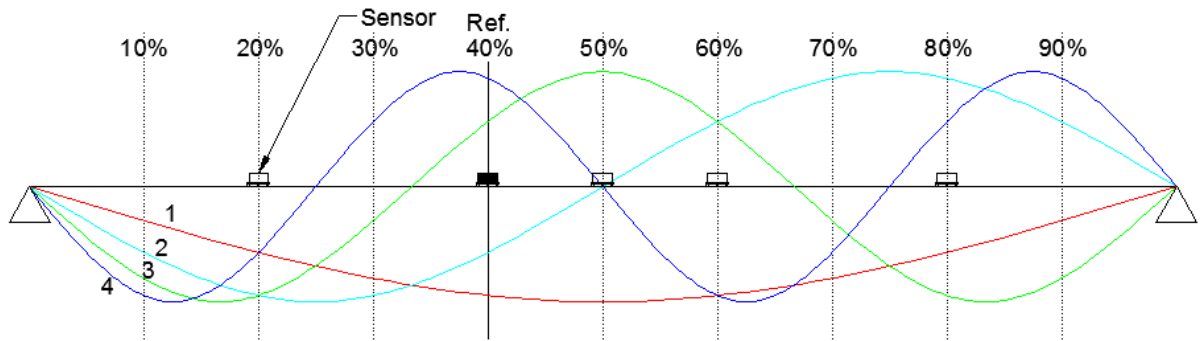


Figure 33: Example layout of glass panel with mode shapes (1st, 2nd, 3rd, 4th)

However, a glass panel is planar component with various side lengths and therefore has different mode shapes in different direction. To cover this, the measurement has to be done in two perpendicular axes which have an intersection at their 40% points. Along those axes sensors were placed to Measure the exact mode shape according to each Eigen frequency.

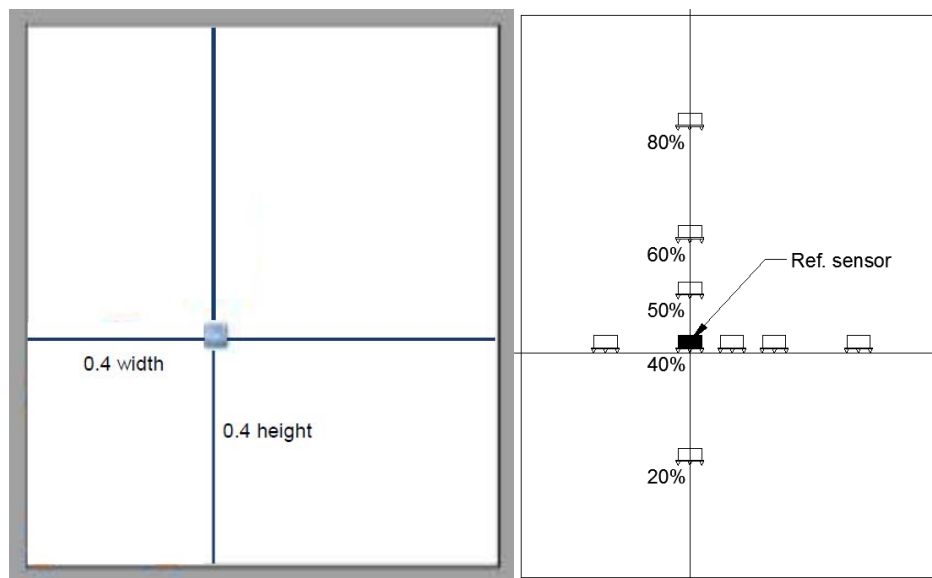


Figure 34: Sensor layout glass panel (right); position of the reference sensor (left)

In case of gold tower the boundary conditions of the panels needed to be investigated so the sensors were placed at the rim of the panel and the rectangle enclosed by the 40% axes was examined closer.

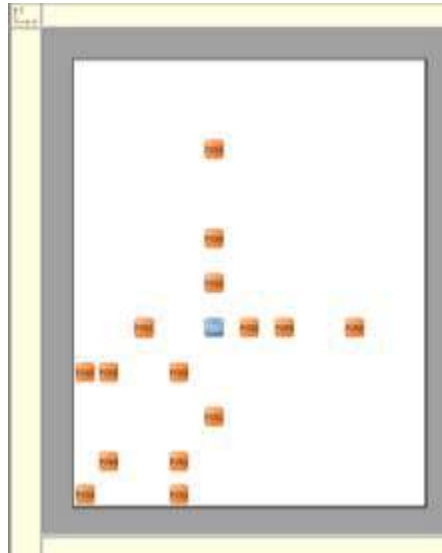


Figure 35: All sensor positions

Another important aspect was the exposure of the measured glass panel. Most of the broken glass panels were located in the middle of the building so for a significant measurement a glass panel in the middle must be measured. Since this is too dangerous for the operating measurement engineer only glass panels within reach of a long ladder have been evaluated.

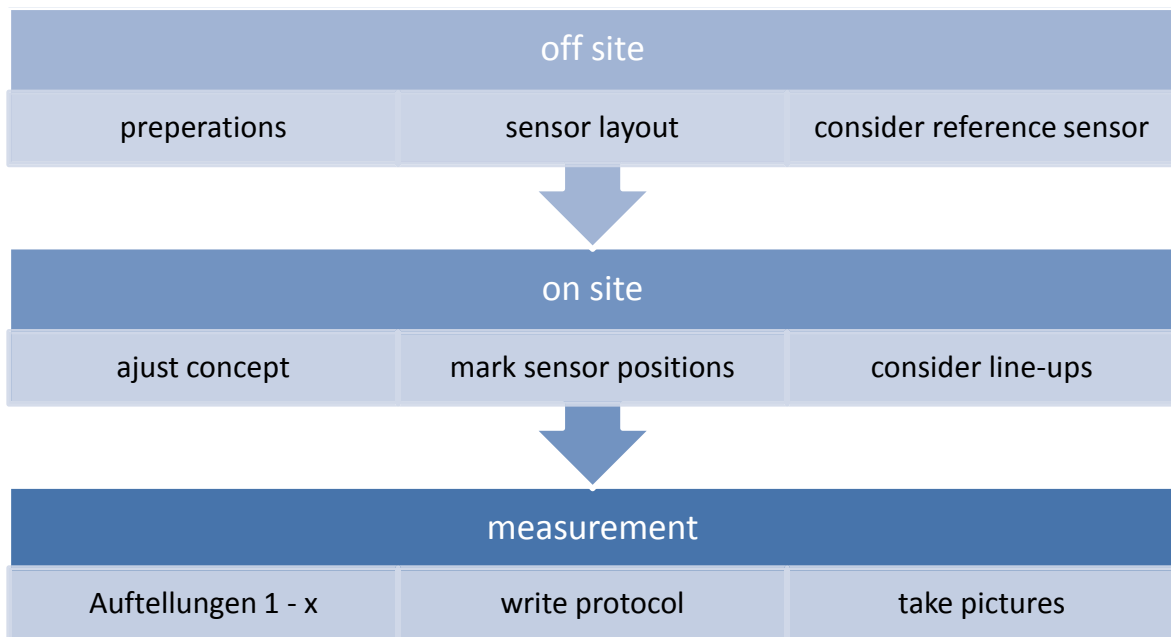
3.3 Execution of a monitoring project

This chapter will describe the process of a monitoring project from scratch to end of measurement. It will explain the basic steps that are needed to accomplish such a project using the BRIMOS Wireless system developed by VCE.

At the beginning of this chapter a definition has to be made. Since it is not economic to bring a sensor, cable and a sensor unit for every sensor position, the sensors (except the reference sensor) has to be moved to different positions during the measurement. When every sensor is at its current location and the data acquisition unit starts to record, that is called a measurement line-up (line-up). Dividing the needed sensor positions through the number of sensors available gives the minimum number of line-ups.

A monitoring project can be outlined in three major steps.

- The off-site work. Which contains mostly preparations considering the FEM model
- The on-site work. Where the concept should be adjusted to the real-life conditions
- The measurement



3.3.1 Off- site work

The off-site work starts with computing the FEM model. The model is set up with the available plan material and information considering the material and loading properties. These documents have to be supplied by the owner of the building. The first FEM model behaves like the building would right after construction without any damages or material flaws. This is used to calculate the Eigen frequencies and mode shapes for creating of the sensor layout.

Creating the sensor layout is the second part of this step which is mostly done by experience. VCE has accomplished over 3000 monitoring projects and out of that experience, developed certain rules for creating the sensor layout and placing the reference sensor. The reference sensor is used to synchronise the data after the measurement. It should always be in a place with relatively big excitations. The layout basically depends on what must be evaluated and to know that VCE again draws on experience. The sensor layout is independent of the used monitoring

system. Any system can be applied at any layout, it's just the amount of equipment that changes.

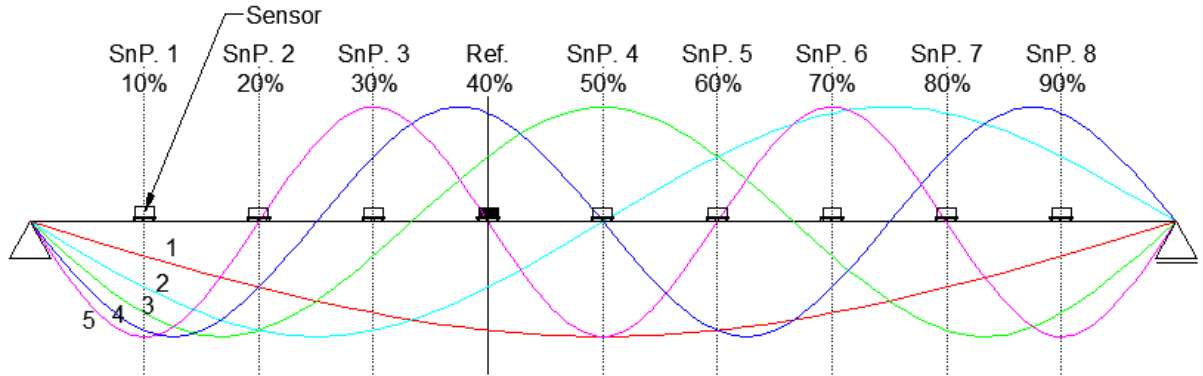


Figure 36: example sensor layout with sensor positions (SnP.) and mode shapes (1, 2, 3, 4 and 5)

Also an important part of the off-site work is the selection of corresponding sensors. The BRIMOS Wireless system can record data from almost any sensor with voltage based output so the selection depends on the sensor attributes. For example for measuring a bridge with a long main span or a tall skyscraper the sensors need to be able to measure very low frequencies in 3 dimensions. This is caused by the high dynamic mass and long distances. On the other hand for measuring a short cable with high tension applied the sensors can be less sensitive to low frequencies and only two dimensional because the vibration along the axis of the cable is not significant.

3.3.2 On-site Work

The on-site work always starts with a quick visual inspection of the building and by setting up a protocol to take notes. If the visual inspection finds any unexpected damage, the sensor layout can be adjusted. After that all planned sensor positions are marked. Since reality and plan doesn't always match, sometimes the sensor positions have to be adjusted. This is noted in the protocol to make sure the right distances are used in the calculations afterwards.

After, all sensor positions are defined, the available equipment is checked and Line-ups considered. To consider Line-ups the number of sensor and sensor units has to be taken into account. The reference sensor is independent of the Line-ups it stays at the exact same spot and measures continuously.

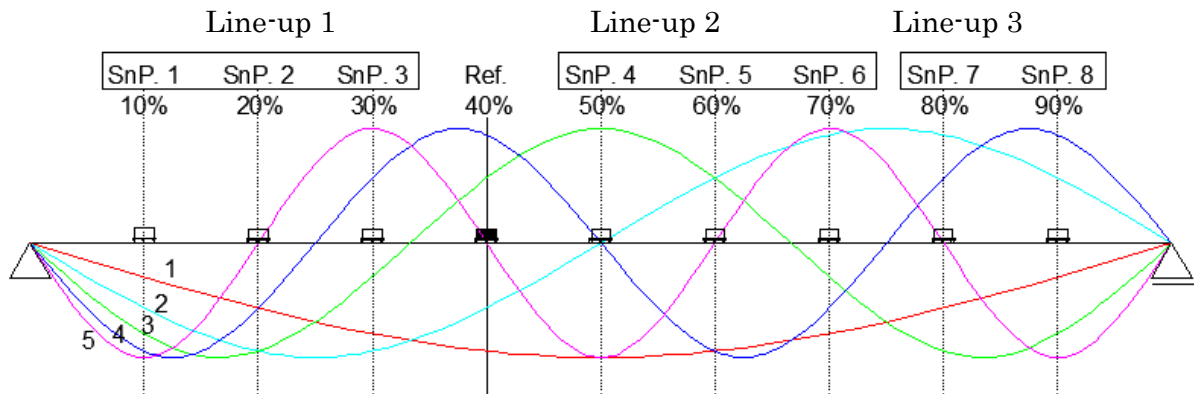


Figure 37: example of a sensor layout with Line-ups, sensor positions (SnP.) and mode shapes (1, 2, 3, 4, and 5)

The picture above shows an example of a measurement with 3 Line-ups. This is done with 2 sensor units and 4 sensors. The reference sensor is stationary and three sensors with one unit move from Line-up 1 to 3. This is a typical BRIMOS Wireless measurement arrangement which spares a lot of equipment.

3.3.3 Measurement

During the measurement writing a protocol is of utter importance. Incidents like for example a very big truck crosses the bridge need to be recorded otherwise it might look like damage in the evaluation afterwards. Also exact sensor positions and serial numbers have to be noted.

To start measuring the sensor units need to be started and synchronised. BRIMOS Wireless works with GPS time, to start the units they must have GPS reception. The starting measurement point and the end of measurement point each unit is synchronised with each other, if not the GPS timestamp makes assembling the data afterwards still possible.

How long the measurement on each Line-up needs to be depends on the expected Eigen frequencies. The smaller the frequency the longer the measurement has to be. Every Line-up is noted in the protocol and pictures are taken from every sensor position. At every Line-up the data collected by the sensor unit is overviewed to check if every component is still working properly.

At the end of the measurement the data is quickly overviewed again and the sensor units shut down.

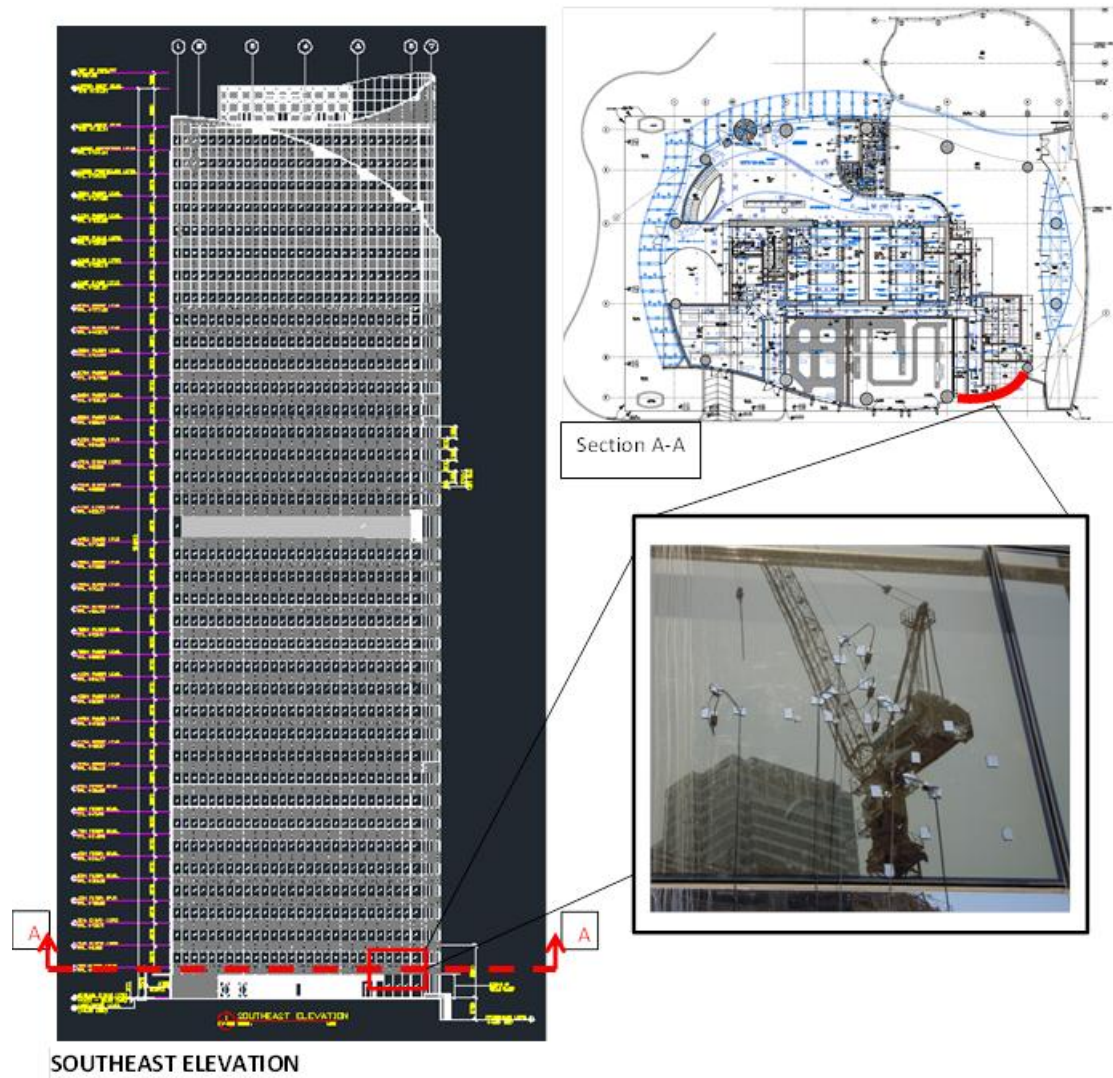


Figure 38: Measured glass element at ground floor

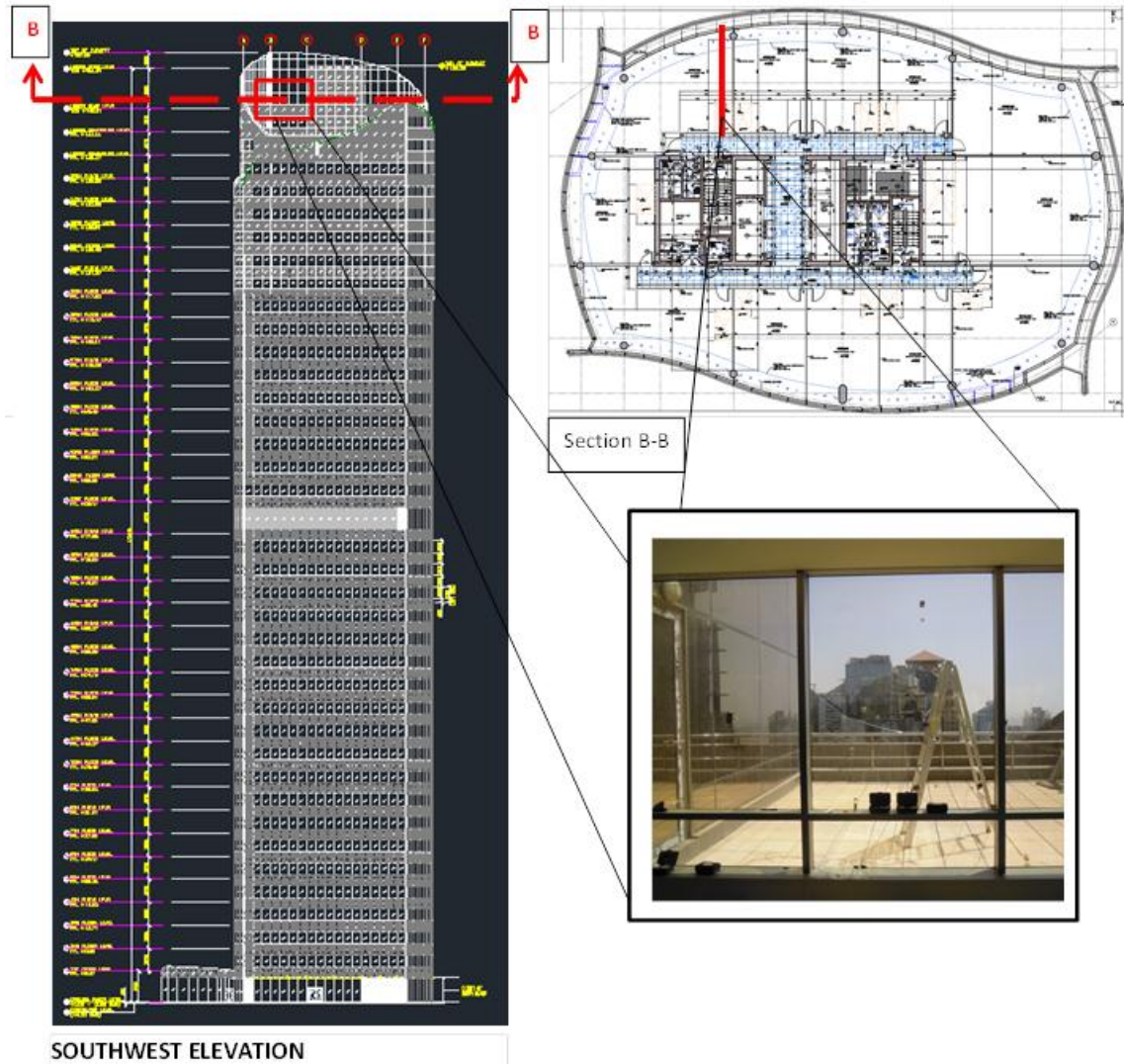


Figure 39: Measured glass element at 35th floor

4 Measurement results

The measurement result in this case is a signal which represents the acceleration of the tower for a certain time and place inside the tower. There was no artificial agitation of the tower which results in so called ambient vibration Monitoring. Such a signal basically looks like Figure 40.

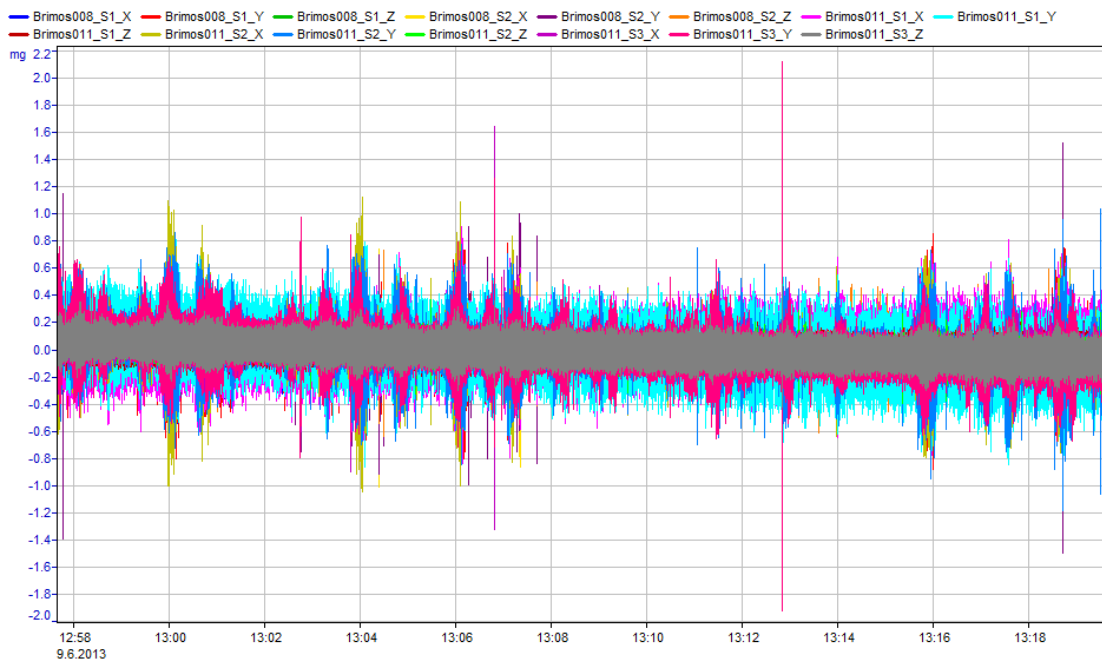


Figure 40: Measurement signal

Each line shows the acceleration in 1 dimension. One 3D sensor therefore needs 3 channels. As explained before a reference sensor was needed to know how to assemble all channels correctly in time.

From this unprocessed data so called “Key Performance Indicators” can be extracted. With these indicators the structural response of the building can be measured. In the following pages a view of these Indicators shall be addressed that are especially important for high rise buildings.

4.1 Key parameters of high rise buildings

4.1.1 Natural Frequencies

The eigenfrequencies – recurring harmonic response in terms of vibration – which are extracted from the measurement signal represent the effective dynamic stiffness of the structure (H. Wenzel, 2005).

In Order to extract the eigenfrequencies of the building the measurement signal has to be processed with a **Fourier-transformation**. Each signal (1D acceleration) is transformed into a Spectrum over a time period.

All these resonance frequencies reflect global response (bending and torsion) linked with the dynamic stressing of the whole high-rise building (H. Wenzel, 2005).

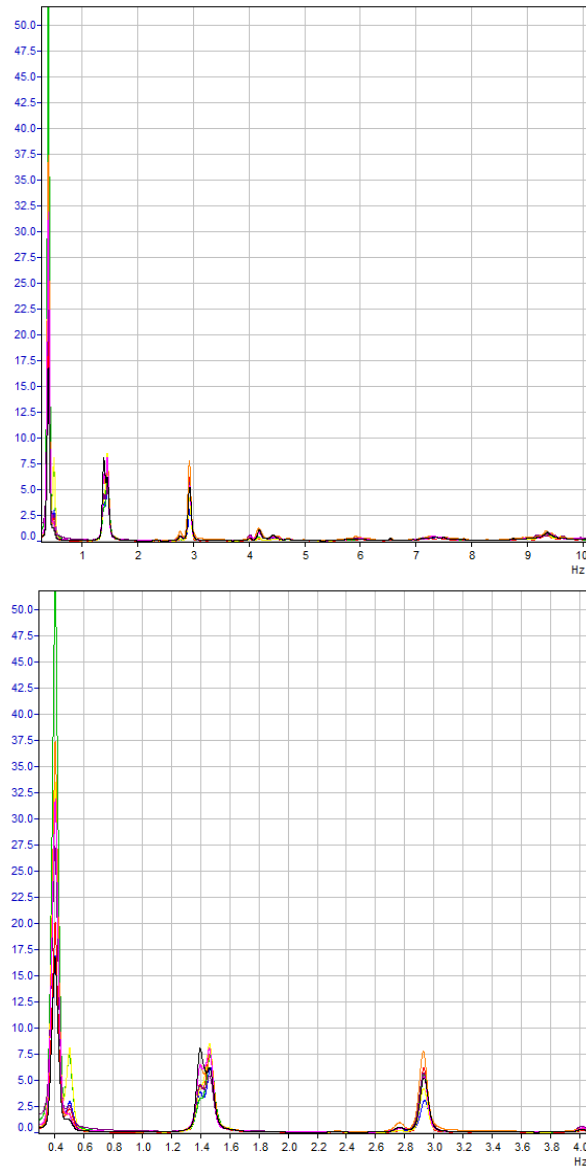


Figure 41: Spectral analysis (ANPSD) for all measurement files, longitudinal direction; 0.3-10 Hz (left) and 0.3 – 4 Hz (right)

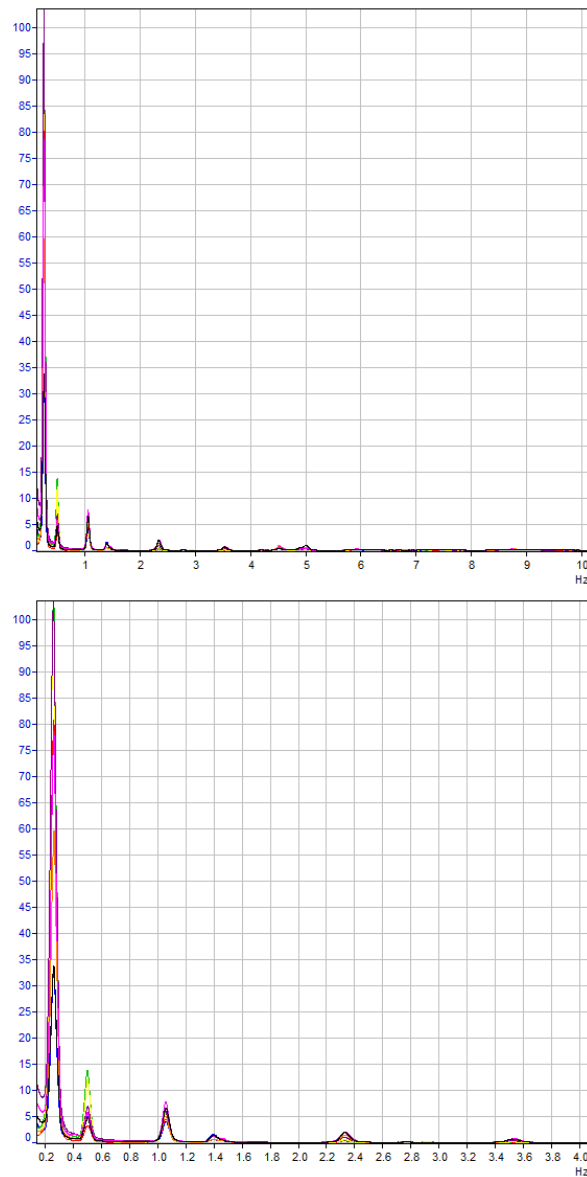


Figure 42: Spectral analysis (ANPSD) for all measurement files, transversal direction; 0.1-10 Hz (left) and 0.1 – 6 Hz (right)

The relevant eigenfrequencies are primarily located between 0.1 and 4.0Hz. The following table (Table 4) shows all identified eigenfrequencies which have been considered relevant for further evaluation. The selection of the relevant frequencies depends on VCE company know-How.

No.	Vibration mode (Kind of loading)	BRIMOS Measurement [Hz]	Spezification regard. Character of Motion and Origin of Stressing
1	1 st bending mode	0,26	1BT - 1 st bending along transversal axis
2	2 nd bending mode	0,40	1BT - 1 st bending along longitudinal axis
3	1 st torsional mode	0,50	1TL - 1 st torsion
4	3 rd bending mode	1,06	2BT - 2 nd bending along transversal axis
5	2 nd torsional mode	1,40	2TL - 2 nd torsion
6	4 th bending mode	1,46	2BT - 2 nd bending along longitudinal axis
7	5 th bending mode	2,34	3BT - 3 rd bending along transversal axis
8	6 th bending mode	2,93	3BT - 3 rd bending along longitudinal axis

Table 4: Natural Frequencies from the measurement at the tower

4.1.2 Mode Shapes

The analysis of the individual mode shapes enables the allocation of the eigenfrequencies to the corresponding motion of the structure. The curvature of the mode shapes is an important parameter for the assessment of the structural integrity and its operational characteristics (e.g. exhibiting highly stressed areas). Furthermore mode shapes enable the identification of changing boundary conditions, e.g. the settlement of the building. Distinctively occurring mode shapes usually indicate a satisfying operability under the given loading (Wenzel, 2009).

The mode shapes are calculated via the 3rd derivation of the measured acceleration (for one sensor at once) which is the moved distance. For this step the reference sensor is of utter importance because it enables the linkage of the sensor movements in time to get the curvature of the building.

The following mode shapes are characteristic mode shapes to be expected in this kind of structure. They correspond to the expected modes of vibration. The colour scale in the provided illustration is of no meaning and is only used for visual reasons.

The determined mode shapes indicate **regular operability**.

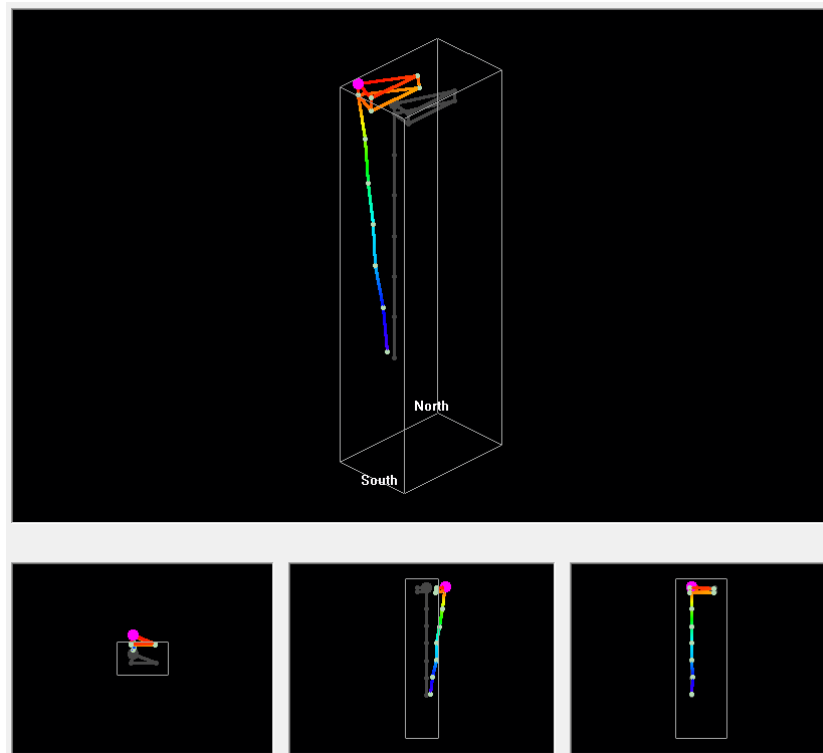


Figure 43: 1st bending mode – 0,26 Hz, 1BT along transversal axis

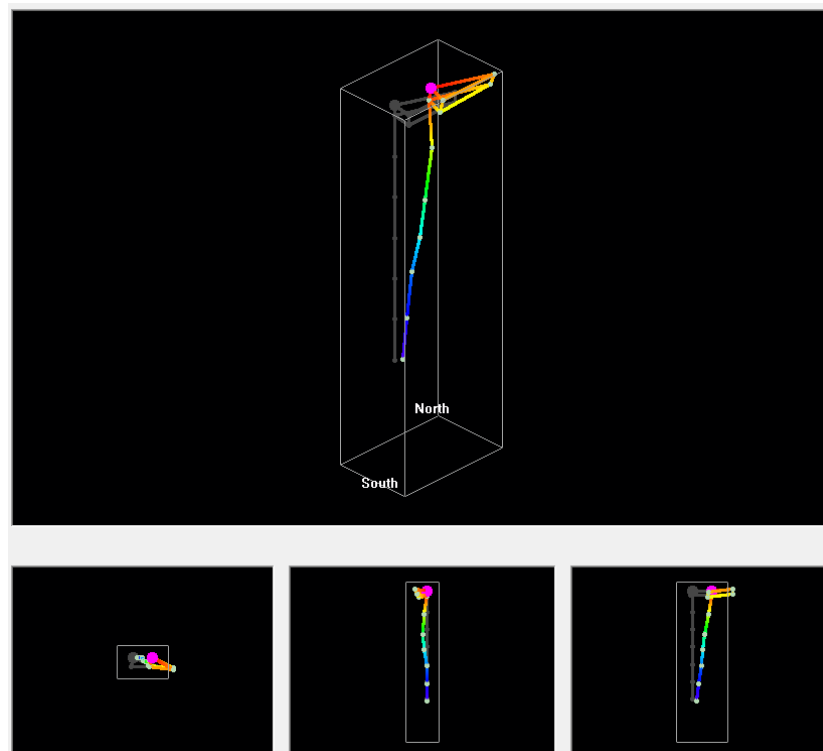


Figure 44: 2nd bending mode – 0,41 Hz, 1BT along longitudinal axis

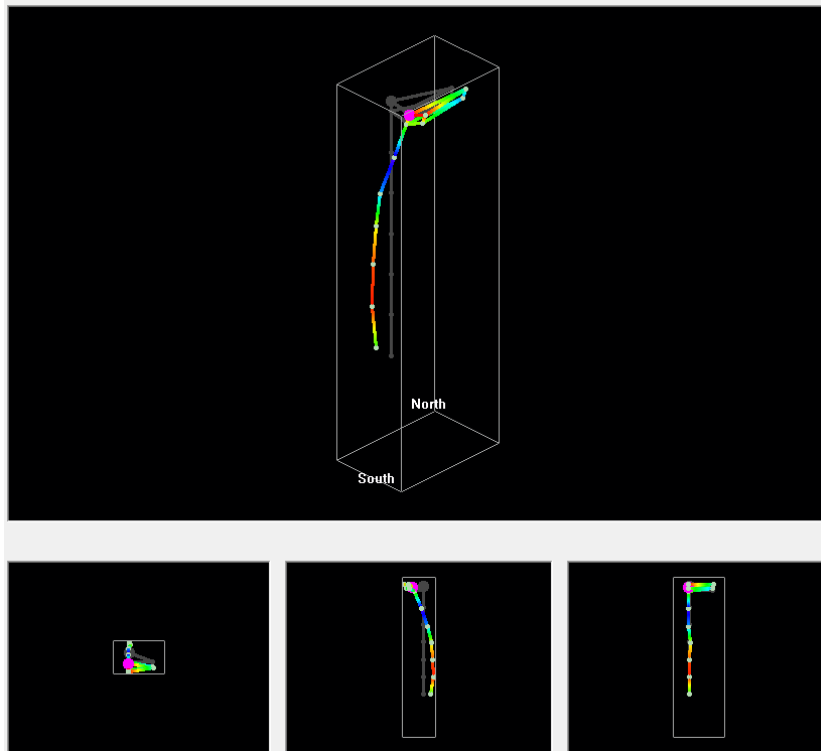


Figure 45: 3rd bending mode – 1,06 Hz, 2BT along transversal axis

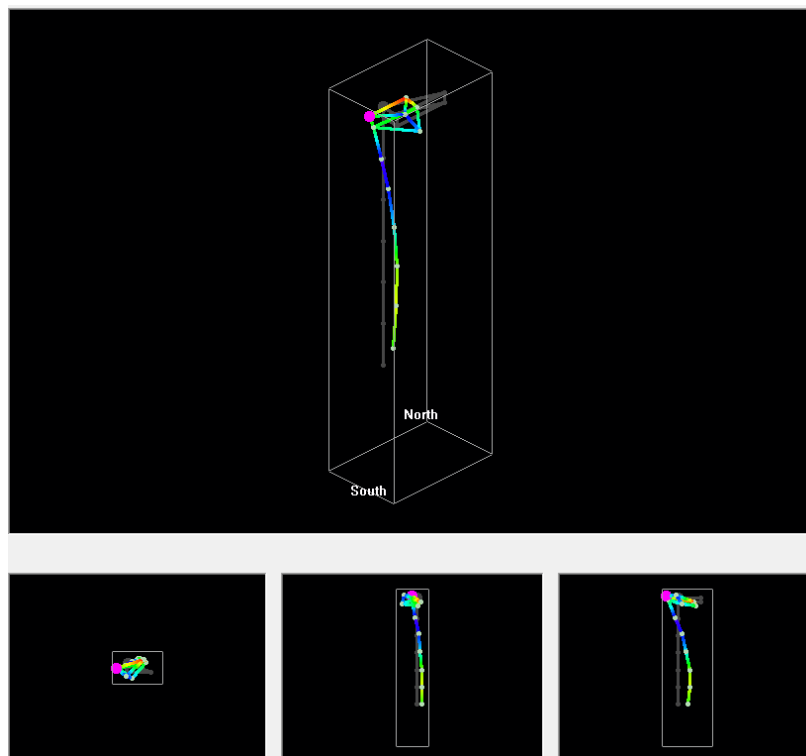


Figure 46: 2nd torsional mode – 1,41 Hz, 2TL

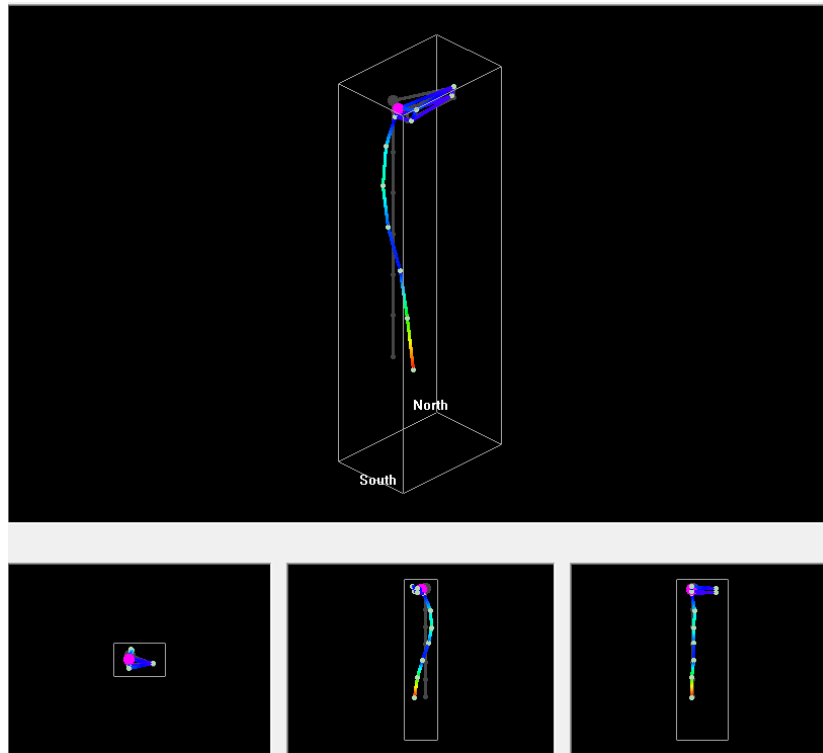


Figure 47: 6th bending mode – 2,34 Hz, 3BT along transversal axis

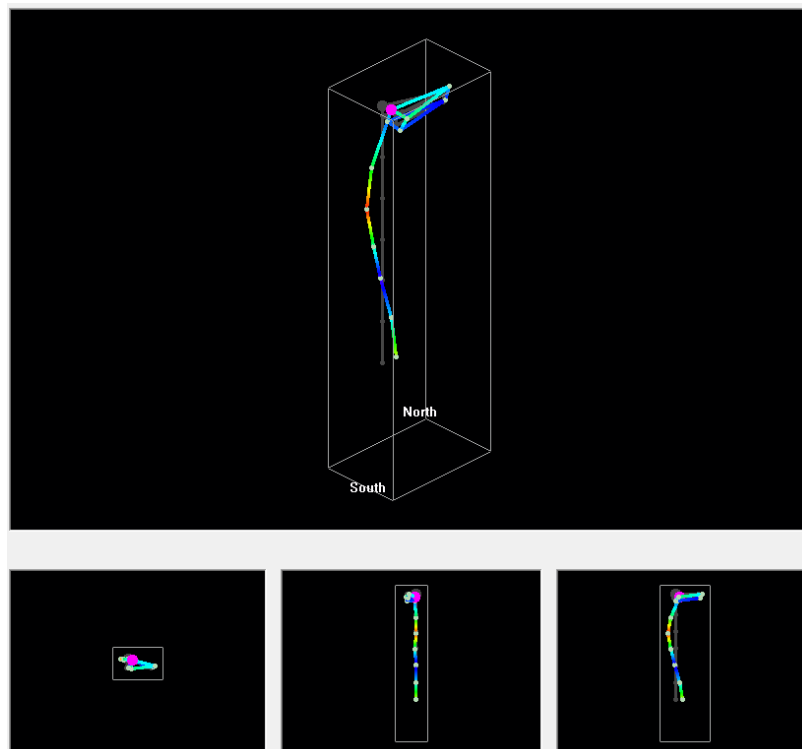


Figure 48: 6th bending mode – 2,93 Hz, 3BT along longitudinal axis

4.1.3 Vibration Intensity

Intensive dynamic loading causes material fatigue-failure. The vibration intensity represents the energy-impact into the analysed structure. The intensity for the investigated building is determined at all sensor positions and included into a diagram, which reflects the corresponding risk level (H. Wenzel, 2005).

The analysis of the vibration intensity evaluates the oscillation amplitude according to its eigenfrequency. Depending on the frequency the value of the amplitude are acceptable or not. A higher frequency permits lower amplitudes and vice versa. *If the oscillation amplitudes exceed certain limits, damage by vibration based overstraining (fatigue) to the structure or to structural elements has to be expected* (Wenzel, 2009).

The vibration intensity is subdivided into 4 zones, ranging from low probability of damage due to dynamic stress (Zone I) up to very high probability of damage (Zone IV) (Beards, 1996).

The measured values of amplitude are exclusively in Zone I for all points of measurement. This indicates a low level of impact in terms of dynamic stressing for the current loading.

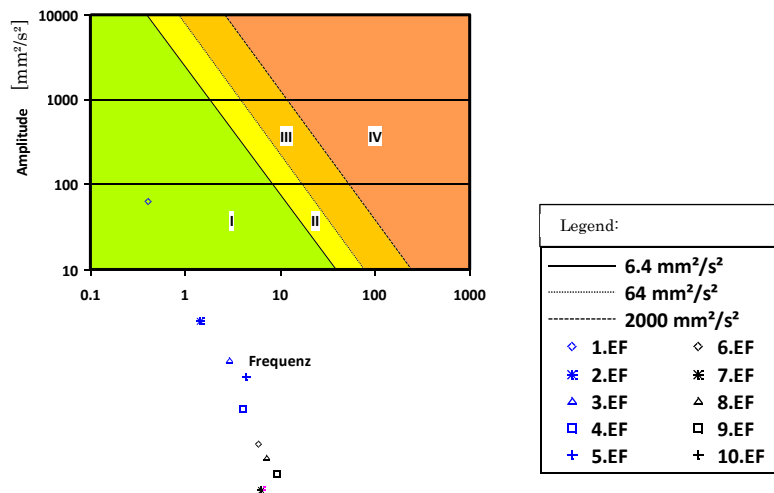


Figure 49: Vibration intensity longitudinal – all points of measurement

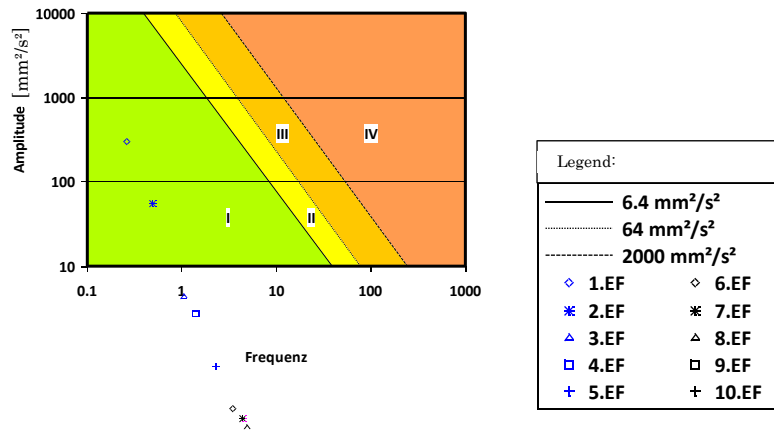


Figure 50: Vibration intensity transversal – all points of measurement

4.1.4 Evaluation of Structural Integrity

Trend cards are an essential evaluation instrument for full-scale measurements on structures. They represent the signal in a frequency-time diagram. It has to be mentioned that very low frequencies with long-wave vibration periods are insensitive to local damage. Therefore the assessment and interpretation of the whole measured frequency spectrum assume greater significance (H. Wenzel, 2005).

The colour coding of the following illustration is depending on the energy content of the oscillation and therefore the respective intensity. It should help to distinguish the individual frequency peaks. If damages occur during the time of observation the peaks jump to different frequencies.

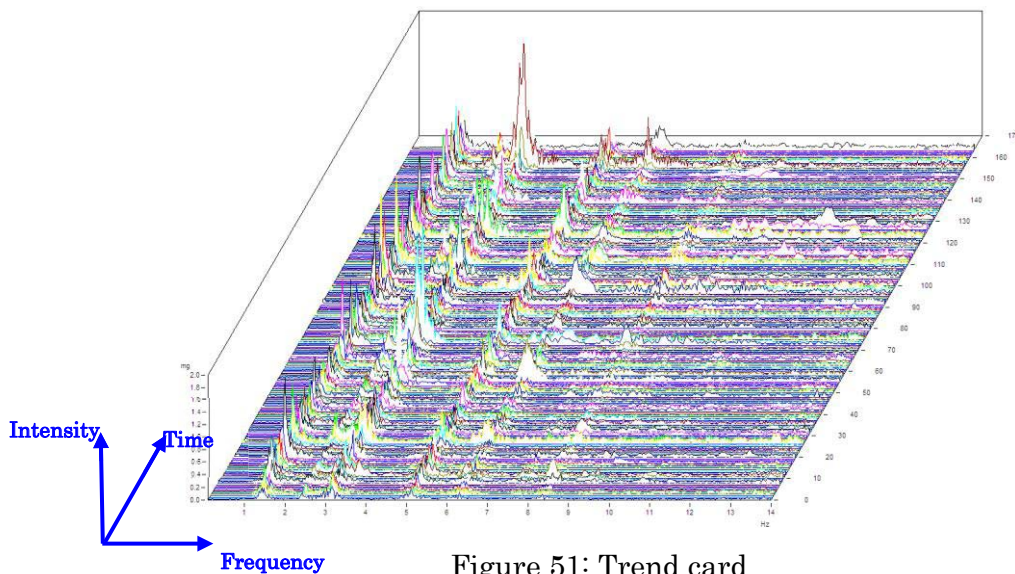


Figure 51: Trend card

The illustration shows frequency spectra for short periods of time aligned in chronological order. The alignment of the peaks, represent the trend of a certain frequency. In the present investigation the trend analysis is executed for a short period of time there for the significance of the trend analysis is doubtful.

Based on the initial dynamic system identification further periodic measurements provide the possibility to study the structure's maintenance condition over time in order to identify remarkable changes of the dynamic structural response. Periodically repeated measurements assures the determination, observation and assessment of slowly progressing processes in the structure, which lead to damage or to deterioration of the structure's operational integrity (H. Wenzel, 2005).

The following trend cards were deprived of the data of the reference sensor because this sensor is the only one measuring the whole time. As was mentioned before, there is no trend due to the short investigation period (1 Day). The cards serve only as examples of how it should look like.

The first card represents the tower's relevant stiffness patterns in longitudinal direction and the second card in transversal direction.

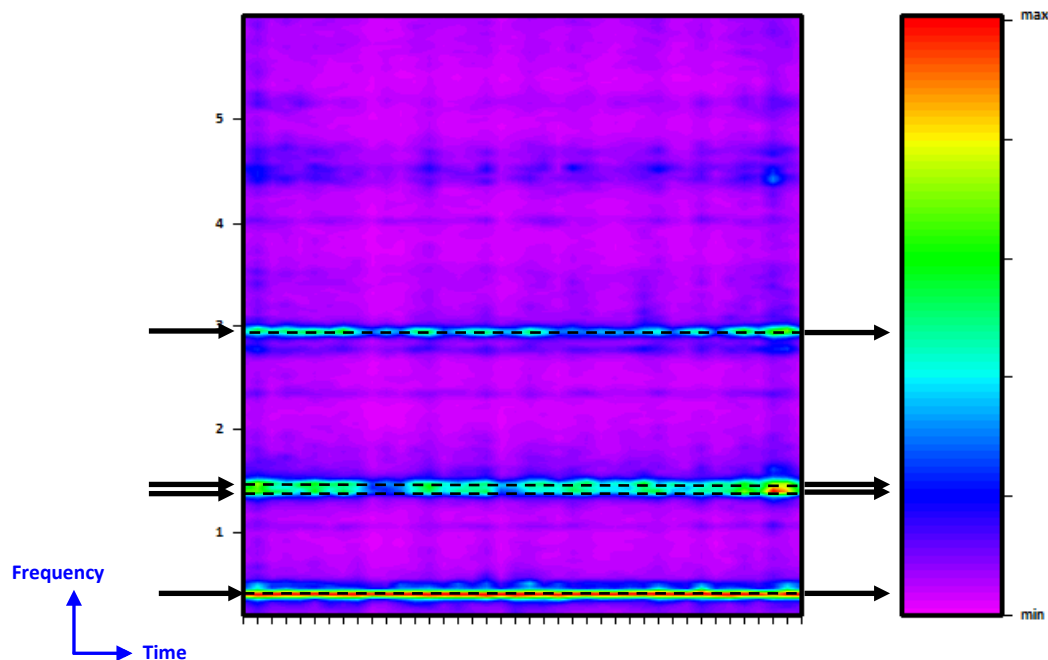


Figure 52: Trend of stiffness distributed over time (entire measurement period), 0,3-6 Hz, longitudinal

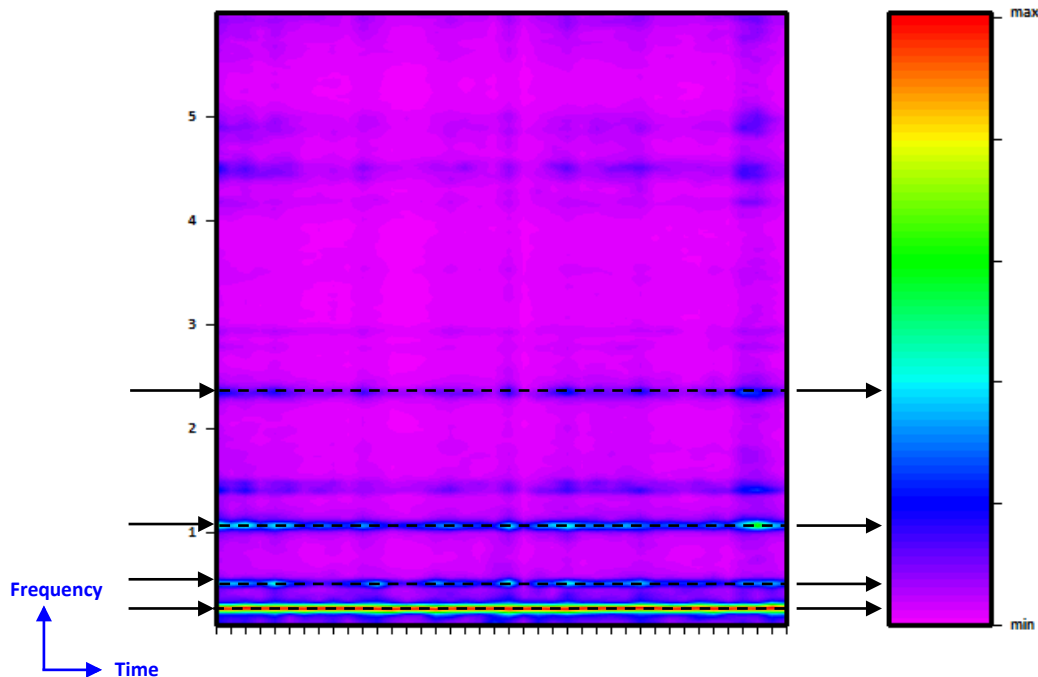


Figure 53: Trend of stiffness distributed over time (entire measurement period), 0,1-6 Hz, transversal

In trend cards for such a short time period there is no global trend visible. High rise buildings are usually climate controlled so the loadbearing structure has always the same temperature and therefore no day temperature impact.

It is possible to compute thresholds for this trend cards in the modelling stage. In this case that has not been done because the trend cards show a not significant time span and there is no further measurement planned. Future trend cards could be compared with this on to guess a trend but it would not differ between damage, fatigue and service life.

4.2 Key parameters of the Glass Panel

4.2.1 Signals

Measuring the glass panels delivers a slightly different signal than the measurement of the whole building. First the used sensors are one dimensional accelerometer and secondly the measurement period is much shorter due to the higher eigenfrequencies. But the procedure with the reference sensor stays the

same. Also the natural excitement (ambient vibration) without artificial intervention is measured.

The following figure (Figure 54) shows a typical measurement signal measured at the tower: the random pattern is due to the ambient vibration.

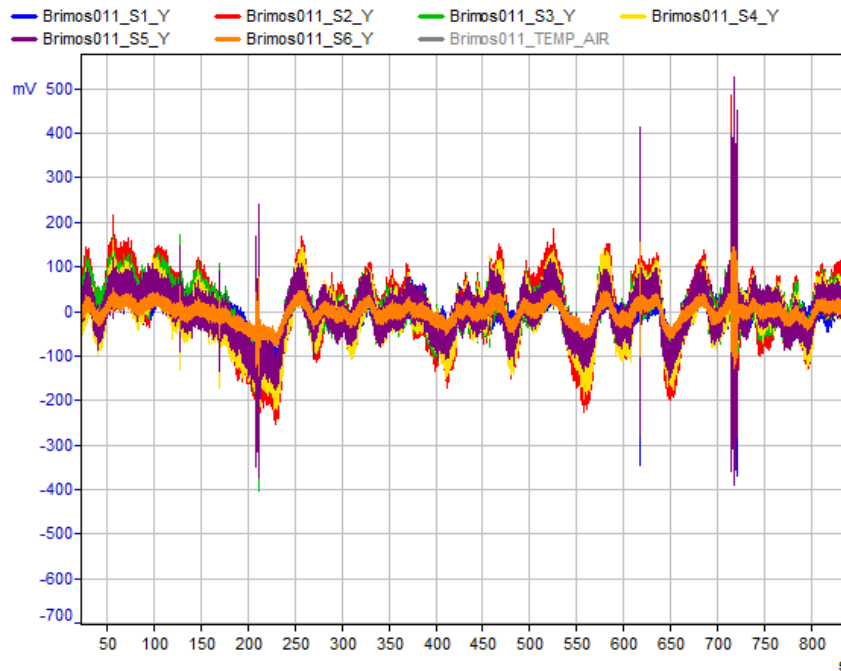


Figure 54: Acceleration signal, all measured channels, façade element 37th floor

4.2.2 Natural Frequencies

As before the signal must be transformed into a spectrum to give values for the eigenfrequencies. The measured spectra show a satisfactory characteristic in the measured dimension (out of plane). The relevant eigenfrequencies are in a range of 20 – 45 Hz of that spectrum.

Due to the given glass-steel composite frame several resonance frequencies with almost the same type of motion but differing frequency values are observed what is to be expected for this type of multi-component structural member (VCE ZT GmbH., 2014).

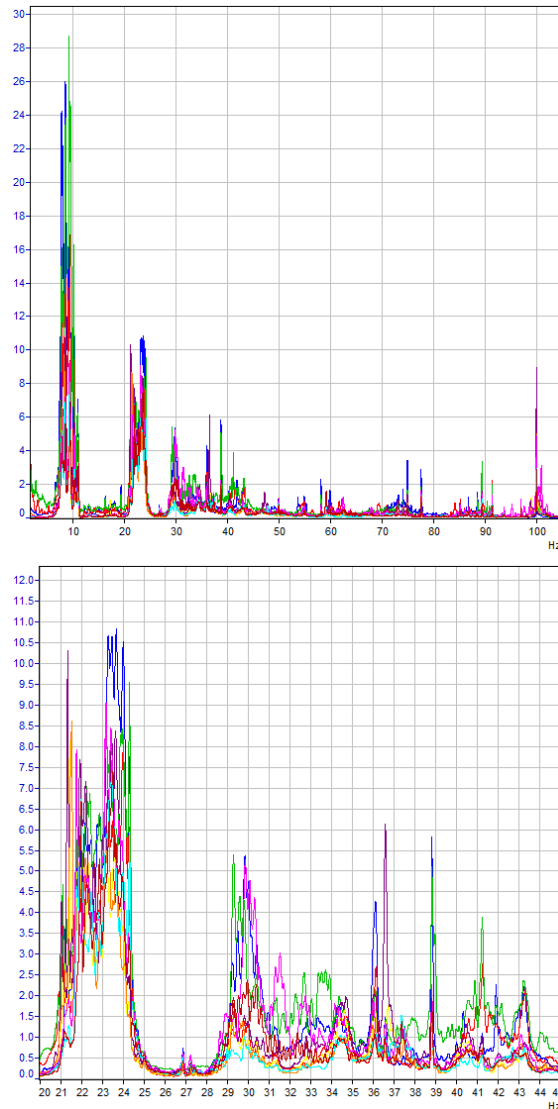


Figure 55: Spectral analysis (ANPSD) for all measurement files (in-depth measurement), out-of-plane; 2-100 Hz (left) and 20 – 45 Hz (right) – Panel 2 (37th floor) exemplarily

4.2.3 Mode Shapes

The measured Mode Shapes correspond to the expected behaviour of this kind of structural member. An illustration of the measured mode shapes is shown in Figure 56 and Figure 57 below. Again the colour scale of the image is of no meaning and is used for visual reasons only.

The determined mode shapes indicate **regular dynamic behaviour** of the glass steel composite frame.

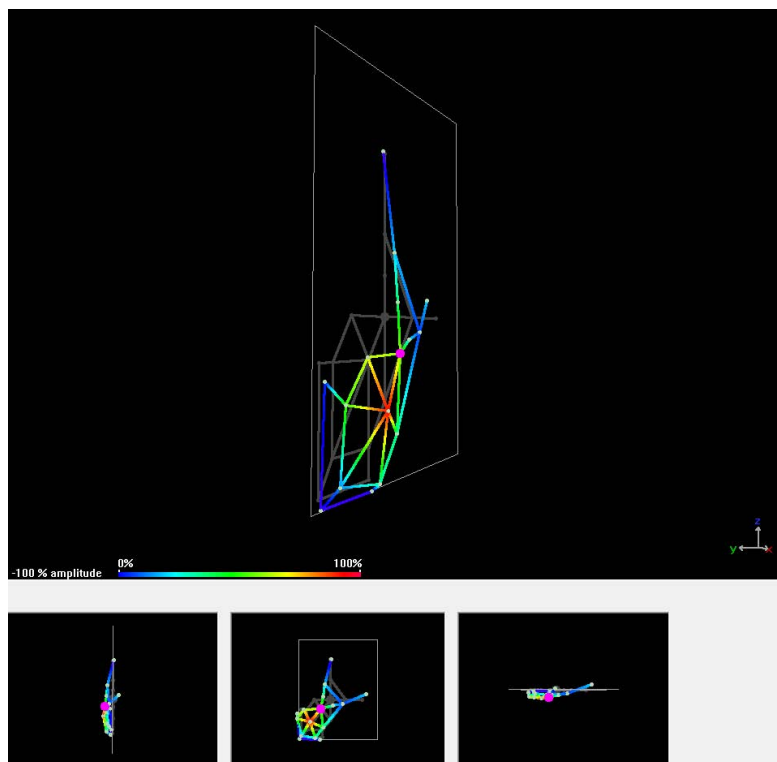


Figure 56: 1st bending mode Panel 2 at 37th floor – 21,94 Hz, 1BT

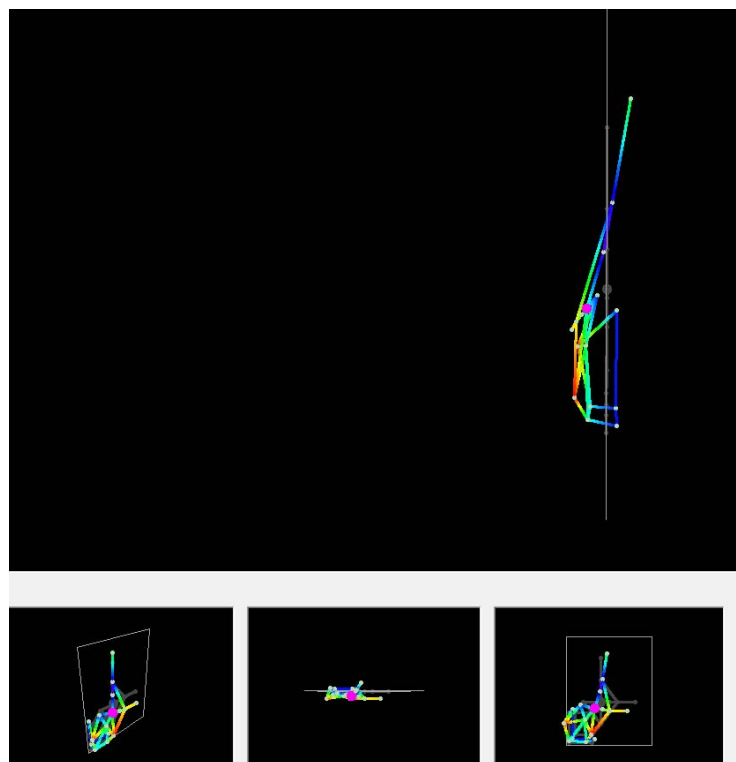


Figure 57: 2nd bending mode Panel 2 at 37th floor – 40,04 Hz, 2BT

4.2.4 Comparison between the measured Panels

The following Table 5 shows the dynamic properties of all measured panels. The comparison between each panel enables to look for damages in single panels and to compare the mounting of the panels.

The comparison of the eigenfrequencies show almost equal value between different panels. The deviation of resonance frequencies between 37th floor and ground floor is a result of the different geometry of the panels. (37th floor: 1500mm X 1900mm; and ground floor: 1500mm X 1786 mm)

37th Floor	Panel 1	
Mode Shape	Measurement Inner Pane [Hz]	Measurement Outer Pane [Hz]
1st Bending Mode	21,89	21,91
2nd Bending Mode	38,81	38,81
	Panel 2	
	Measurement Inner Pane [Hz]	Measurement Outer Pane [Hz]
	-	21,94
	40,04	40,04
	Panel 3	
	Measurement Inner Pane [Hz]	Measurement Outer Pane [Hz]
	21,76	21,56
	39,13	39,13
	Panel 4	
	Measurement Inner Pane [Hz]	Measurement Outer Pane [Hz]
	21,79	21,69
	38,81	38,81
	Panel 5	
	Measurement Inner Pane [Hz]	Measurement Outer Pane [Hz]
	21,8	21,8
	38,82	38,82
	Ground Floor	
	Panel 6	
		Measurement Outer Pane [Hz]
		21,42
		38,27

Table 5: Eigenfrequencies from the measured glass façade elements

4.3 Additional investigation of the glass elements

Additional to the measurement campaign, data has been acquired from the client about the preceding damages of the glass elements. This data gives a distribution of broken panels over time and cardinal direction. Temperature and wind speed data was also acquired for the same time frame. The meteorological data has been acquired from (www.wunderground.com).

This data is covered in chapter 4.3.2 Long term observations.

Also the critical buckling resistance of the single glass pane has been calculated. This gives a perspective on how likely this kind of failure is.

4.3.1 Buckling stress of façade elements

The following chapter is based on (Petersen, 1980).

Buckling stress can be the cause of glass failure in this case. It is assumed that the building movement results in high normal forces applying to single façade elements. This can cause buckling failure.

To calculate the maximum buckling stress certain assumptions has to be made. The updated FE model gives a very specific description of the boundary conditions. It is not possible to calculate these exact conditions with the used method and by hand therefore the conditions will be simplified. But always in the unfavourable direction to make sure the resulting max buckling force is not bigger than the one with the actual boundary conditions.

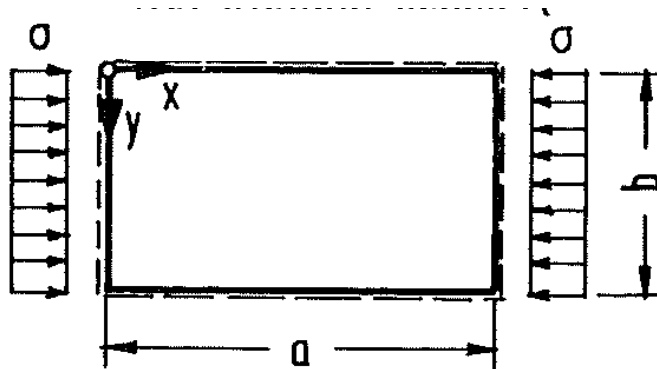


Figure 58: Boundary conditions used for calculation (Petersen, 1980)

The edges are not fully clamped as they are in the model. The used conditions result in lower buckling resistance compared to the modelled conditions so the result is on the safe side.

The following diagram helps to determine the critical buckling shape. This can be directly compared to the mode shapes. The diagram shows curves with negative apexes. Those curves represent the buckling value which directly correlates to the buckling resistance. This value is dependent on the geometric shape of the plane element.

$$\alpha = \frac{a}{b} \tag{4.1}$$

a = the length of the long side of the element (in this case 1900mm at the 35th floor and 1786 mm at ground floor) b = the width of the element (in this case 1500mm for both floor planes). $\alpha = 1,27$ for 35th and 1,19 for ground floor elements.

Secondly the buckling value is determined by the loading $\psi=1$.

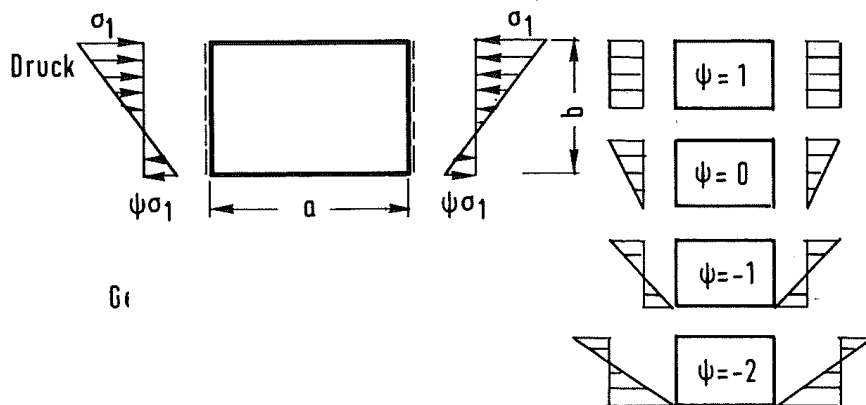


Figure 59: description of ψ (Petersen, 1980)

These two variables are used to determine the buckling value. For the chosen boundary conditions the buckling value can be extracted from the following diagram.

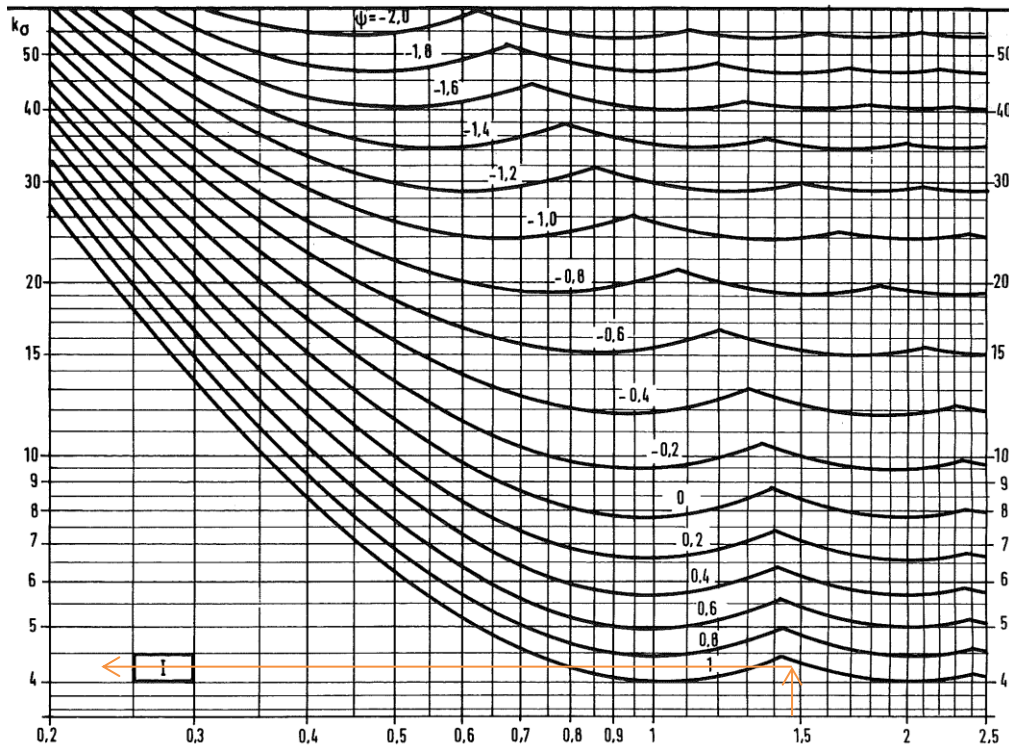


Figure 60: Buckling value k (Petersen, 1980)

Both glass panels hit the curve at the first negative apex which means, the first buckling shape (similar to the first mode shape) is critical. Also the buckling resistance of the smaller glass element located in ground floor has lower resistance. This information is now implemented in the further calculation.

The following equation calculates the buckling resistance stress of a rectangular plane with the above described boundary conditions.

$$\sigma_{KI} = \frac{E\pi^2}{12(1-\mu^2)} \left(\frac{t}{b}\right)^2 * \left(\frac{mb}{a} + \frac{a}{mb}\right)^2 \quad (4.2)$$

σ_{KI} is the critical buckling stress. It is calculated with the material parameters E (elastic module of glass: 7000 kN/cm²) and μ (poisson's ration of glass: 0,23). The values a , b , and t are geometric parameters describing the element. The variable t stands for the thickness of the plane, a and b are the length and width whereas a is always the longer side because that represents the critical load case. The value m describes the calculated buckling shape (in both cases $m=1$). This is determined by the buckling value described above. The buckling value can also be used in this equation but only with a loss of accuracy due to the readout of the diagram.

$$k = \left(\frac{m b}{a} + \frac{a}{m b} \right)^2 \quad (4.3)$$

The last term of (4.2) represents the buckling value k which can also be extracted from Figure 60.

As mentioned before the ground floor plane was the critical one because of its shorter length. The result of the equation for the critical element is:

$$\sigma_{KI} = 5458258,05 \text{ N/m}^2 \Rightarrow 5,46 \text{ N/mm}^2$$

This equals an applied line load of $38207,80 \text{ N/m} \Rightarrow 38,21 \text{ kN/m}$

This value is very high. The construction of façades usually prevents normal forces applying to the glass elements by special glass fixing. If in this case such high normal forces apply to the single element the construction of the façade is fundamentally flawed.

To measure if this failure mechanism is responsible in this case additional measurements would be necessary.

4.3.2 Long term observations

Figure 61 shows a distribution of the occurring damages over time and cardinal direction.

Figure 62 shows the comparison of the glass panel damage history underlying the meteorological conditions including wind speed and temperature.

1. A high number of damages occurred in the first 16 months after completion of the façade. In the meantime the number of occurrences per season has stabilized to a lower level.
2. The damages normally occur in seasons of higher temperatures caused by solar irradiation. The clear correlation between temperature and damage occurrence underlines the contribution of **temperature constrains** to the cracking of glass panels.

In Figure 62 the correlation between temperature and glass failure is clearly visible. Glass failure only happens in summer when the air temperature and solar irradiation is highest. Furthermore the number of failing glass elements decreases dramatically over time, which indicate production failure of the glass.

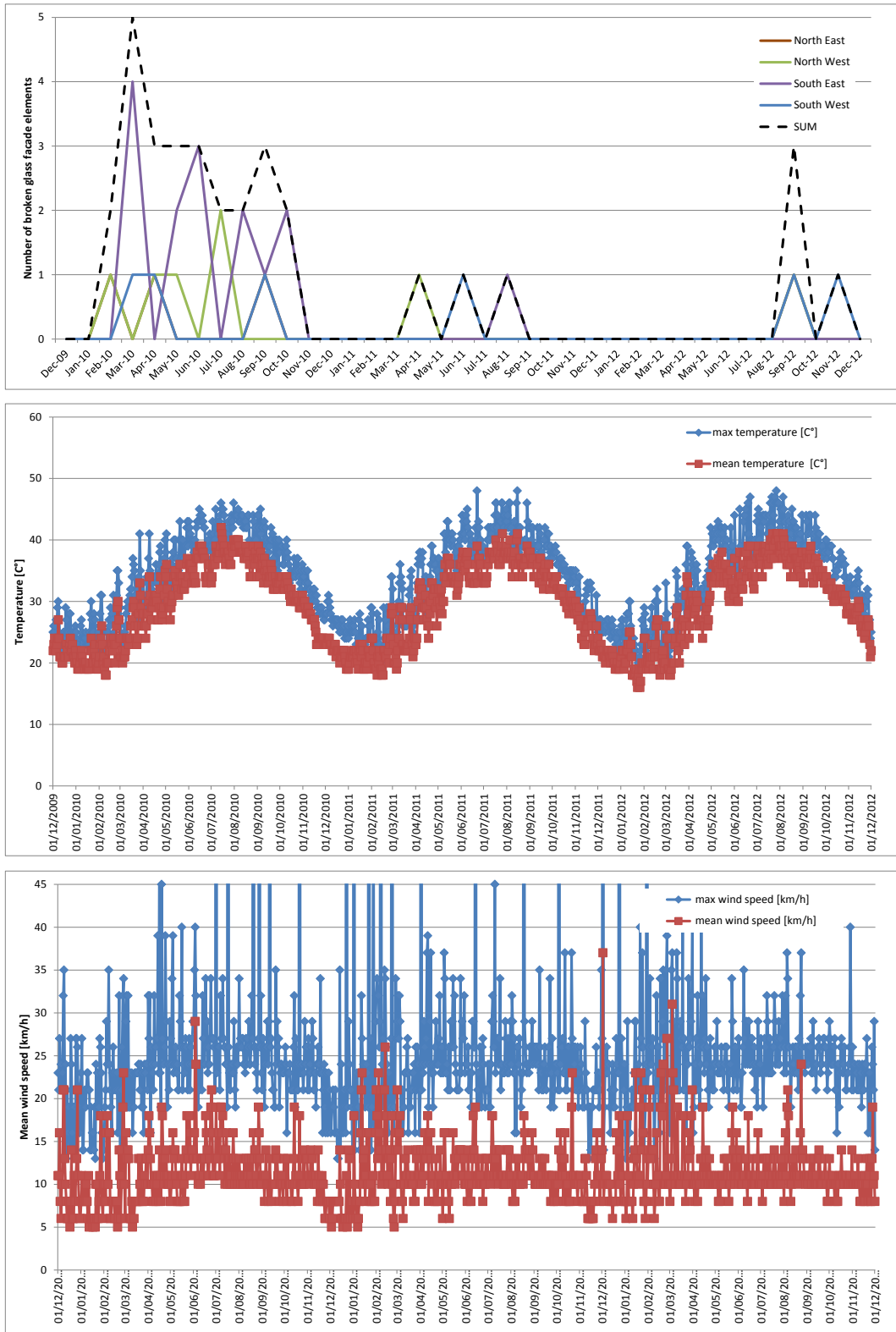


Figure 62: Distribution of broken glass façade elements (top) compared to meteorological data (temperature (middle) and wind speed (bottom))

5 Comparison of Measurement and Simulation

5.1 Tower Structure

Before the measurement and the model can be compared the model has to be updated to better represent the actual conditions of the building. In case of the tower the model update was done by a VCE employee. This process depends mostly on experience and VCE has special know-how on this matter.

Basically the material parameter and boundary conditions are modified until the model represents the reality conducted by the measurement. This is done by matching the 1st bending mode eigenfrequency.

The following Table 6 shows already updated model parameters. All still existing differences are caused by a divergence from the expected behaviour of the building.

No.	Vibration mode (Kind of loading)	BRIMOS Measurement [Hz]	Updated FE-Model [Hz]	Deviation [%]	EI CG	Spezification regard. Character of Motion and Origin of Stressing
1	1 st bending mode	0,26	0,27	-2	96%	1BT - 1 st bending along transversal axis
2	2 nd bending mode	0,40	0,39	4	108%	1BT - 1 st bending along longitudinal axis
3	1 st torsional mode	0,50	0,67	-33	57%	1TL - 1 st torsion
4	3 rd bending mode	1,06	1,23	-16	74%	2BT - 2 nd bending along transversal axis
5	2 nd torsional mode	1,40	1,72	-23	66%	2TL - 2 nd torsion
6	4 th bending mode	1,46	1,65	-13	78%	2BT - 2 nd bending along longitudinal axis
7	5 th bending mode	2,34	2,76	-18	71%	3BT - 3 rd bending along transversal axis
8	6 th bending mode	2,93	3,28	-12	80%	3BT - 3 rd bending along longitudinal axis

EI ... effective bending stiffness of the tower (modulus of elasticity x area moment of inertia of cross section about neutral axis)

CG ... effective torsional stiffness of considered span (torsional constant of cross section x Shear modulus)

Table 6: Comparison of measurement and numerical simulation – Gold Tower

The calculated parameters (Updated FE-Model) serve as expected values based on undamaged condition. They provide an enhanced insight on the structural dynamic behaviour.

The comparison between numerical simulation and measurement after the FE-model updating shows that the measured fundamental bending eigenfrequencies reflecting global bending (along transversal and longitudinal axis) are in good

agreement with the calculated ones. In other words the global stiffness of the real structure can be assumed to reflect the theoretical one (VCE ZT GmbH., 2014).

The high frequency range reflects more and more local stressing (torsion and higher bending modes). In this frequency band the behaviour is less stiff than it should be. Lower frequencies mean less stiffness and bigger movements. This could result in a redistribution of internal forces from the primary load bearing structure (the core) to the façade elements.

5.2 Glass Façade Elements

Again before the comparison is valid the model has to be updated. It turned out that the boundary conditions at the edge of the panels had to be modelled very stiff in order to achieve reasonable results comparing with the measured values. In other words the boundary conditions of the glass panels can be assumed: **fully clamped**.

The higher frequency values of the measurement compared to the model indicate again increased stiffness due to **local constraint forces**.

37th Floor					
Mode Shape	Panel 1				
	Measurement Inner Pane [Hz]	Measurement Outer Pane [Hz]	Model [Hz]	Δ_{INNER} [%]	Δ_{OUTER} [%]
1st Bending Mode	21,89	21,91	20,40	6,81	6,89
2nd Bending Mode	38,81	38,81	35,50	8,53	8,53
Average deviation				7,67	7,71
Panel 2					
	Measurement Inner Pane [Hz]	Measurement Outer Pane [Hz]	Model [Hz]	Δ_{INNER} [%]	Δ_{OUTER} [%]
	-	21,94	20,40	-	7,02
	40,04	40,04	35,50	11,34	11,34
				11,34	9,18

Table 7: Comparison of measurement and numerical simulation – glass façade elements

Mode Shape	Panel 3				
	Measurement Inner Pane [Hz]	Measurement Outer Pane [Hz]	Model [Hz]	Δ_{INNER} [%]	Δ_{OUTER} [%]
1st Bending Mode	21,76	21,56	20,40	6,25	5,38
2nd Bending Mode	39,13	39,13	35,50	9,28	9,28
Average deviation				7,76	7,33
	Panel 4				
	Measurement Inner Pane [Hz]	Measurement Outer Pane [Hz]	Model [Hz]	Δ_{INNER} [%]	Δ_{OUTER} [%]
	21,79	21,69	20,40	6,38	5,95
	38,81	38,81	35,50	8,53	8,53
				7,45	7,24
	Panel 5				
	Measurement Inner Pane [Hz]	Measurement Outer Pane [Hz]	Model [Hz]	Δ_{INNER} [%]	Δ_{OUTER} [%]
	21,80	21,80	20,40	6,42	6,42
	38,82	38,82	35,50	8,55	8,55
				7,49	7,49
Ground Floor					
	Panel 6				
		Measurement Outer Pane [Hz]	Model [Hz]		Δ_{OUTER} [%]
		21,42	20,67		3,50
		38,27	37,68		1,54
					2,52

Table 8: Continuation of Table 7

37th floor (5 panels comparison) Dimension 1500 mm x 1900 mm

Ground floor (1panel) Dimension 1500 mm x 1786 mm

6 Interpretation of Measurement Results

The aim of this project was to find out why certain glass panels are failing. In this chapter possible reasons of failure are listed the findings of the measurement summarised and a conclusion will be presented.

6.1 Potential Risks for Glass Panel Breakage at High Rise Buildings

Potential sources of glass panel breakages at high rise buildings are:

1. **Nickel Sulphide Inclusions:**

inherent in the glass production process are microscopic imperfections in the glass, known as inclusions. Most of these are completely harmless, but nickel sulphide (NiS) inclusions have been shown to cause disastrous failures of tempered glass. When annealed (aka float) glass is heated in the tempering process, so are any NiS inclusions present in the glass. However, when the glass is rapidly cooled to achieve the properties of tempered glass, the NiS remains in a high-temperature form. Over several years, the NiS will return to its low-temperature state, and in the process will increase in volume (Swain, 1981).

This can cause cracking and additional tensile stresses which, in tempered glass, have led to spectacular failures with no visible cause. This phenomenon has also been referred to as “glass cancer” and “spontaneous glass failure”. The main risk this poses to the building industry comes from in-service failure of window panels containing tempered glass with NiS inclusions. When these windows break, they shatter into thousands of pieces which can fall from panes and cause injury to inhabitants of the building or pedestrians around it.

2. **Damages of Edges:**

The edges are the weakest zone of a glass panel. The cutting of the glass panels may cause micro-damages which considerably reduce the load bearing capacity of the glass. Transport and installation may also cause such defects.

3. **Colouring and Temperature Effects:**

Temperature effects, especially temperature differences, could lead to

high restraints and bending load of the glass. High outside temperatures in combination with high sun radiations lead to an expansion of the outer glass while the inner glass and the curtain wall are cooled down by the air condition. This effect may be amplified by the colouring of the glass.

4. **Restraints of the Panels:**

Problems in the design and with installation of the façade elements. Restraints and temperature effects could cause the sudden breakage of single elements.

5. **Structural Behaviour of the Tower Structure:**

A potential “soft” behaviour of the tower can cause too big deformations of the glass façade elements. If the tower is very slender and the core of the tower, which provides the shear stiffness, shows only a small cross section, the tower could show bending and torsion movements.

6. **Damage by Cleaning:**

Inappropriate cleaning of the glass is a reason for micro scratches in the surface which weakens the glass.

7. **Other External Sources:**

Strong winds in combination with small stones and sand could also be a reason.

6.2 Findings of the Investigation of the Gold Tower with BRIMOS®

The investigation by VCE only focuses on the structural behaviour of the tower structure and possible dangerous restraints caused by the curtain wall and the installation and fixing technology of the glass panels. Other potential sources for the glass breakages are not in the scope of the investigations.

6.2.1 Findings for the Tower Structure

- The dynamic behaviour of the tower structure was measured and compared with a dynamic FE-model of the tower. The performed numerical analysis provides an enhanced insight into the structural dynamic behaviour. The calculated parameters serve as expected values based on the undamaged condition.
- The comparison of the natural frequencies between numerical simulation and measurement are in good agreement for the fundamental bending modes (1st and 2nd). The fundamental bending eigenfrequencies reflecting global bending indicate a regular global stiffness of the tower.

- The measured higher bending modes and especially all the measured torsional modes are considerably lower than the results of the FE-model. This leads to the conclusion that the measured tower stiffness in terms of local bending and torsional stressing is lower than the calculated one from the numerical model.
- This soft behaviour leads to small torsional movements of the tower which generate small movements and stresses in the curtain wall. This can lead to dangerous stresses in the glass panel.
- It is assumed that this fact causes a redistribution of the internal forces from the primary load-bearing structural elements of the tower to local elements like the glass façade elements.

6.2.2 Findings for the Curtain Wall and the Glass Panels

- The comparison of the response frequency values shows almost equal values for different measured panels.
- The deviation between the resonance frequencies on the 37th floor and on the ground floor is given by slightly differing geometric properties.
- During the modelling of the glass panels it turned out that the implemented rotational springs along the glass panel edges are to be modelled very stiffly in order to achieve reasonable results with regard to the measured values. In other words the boundary conditions of the glass panel can be assumed to be fully clamped.
- The comparison of the results from field test and numerical model shows higher frequency values of the measured glass panels indicating increased stiffness due to local constraint forces.
- The comparison of the number of glass breakage per period with meteorological data shows that the glass façade elements normally burst in seasons with higher temperatures.
- The correlation of the number of bursting glass façade elements during seasons with high temperatures and high solar irradiation underlines that additional temperature constraints are a contributing factor causing the breakage of single glass façade elements.
- A high number of glass façade elements broke within the first 16 months after the completion date. In the meantime the number of occurrences per season has stabilized on a lower level. This decrease is typical for glasses with nickel sulphide inclusions.

6.3 Conclusions

The investigations of the Gold Tower based on dynamic measurements and simulations of the tower structure and the glass panels lead to following conclusions:

1. There is not a single reason to be blamed for the glass breakages at the façade of the Gold Tower. A number of factors with negative influences on the glass panels were identified by the investigation. The combination of these factors causes high stresses in the glass.
2. The fixation method of the glass elements to the curtain wall causes high restraints in the glass panel. This makes the glass more vulnerable against additional constraint forces. Global deformation or Temperature effects, especially temperature elongations of the glass, can generate considerable stresses in the glass.
3. The tower structure is considerably softer than expected especially for the torsional behaviour. Dynamic tower movement, e. g. caused by wind, can induce deformations of the curtain wall leading to stresses in the glass.
4. There might be problems with the glass itself. This can only be verified by detailed investigations of the glass. Glass analysis reports have not been available to VCE.

References

- ANSYS. (2012). *ANSYS Manual*.
- Baytur. (2014). Von http://www.baytur.com.sa/DMCC_info.htm abgerufen
- Beards, C. F. (1996). *Structural Vibration Analysis and Damping*. London, GB: Arnold (A Member of the Hodder Headline Group).
- Belvins, R. D. (1979). *Formulas for natural frequency and mode shape*. New York: Van Regional Company.
- Caramelli, S., & Croce, P. (2010). *Influence of heavy traffic trend on EC1-2 load models for road bridges*. Rom: Frascati ENSA Research Centre.
- CESTEL. (2008). <http://www.siwim.com>. abgerufen am 01.2012.
- FS5, E. C. (2006). F08a Guidelines for the assesement of existing Structures/ F08b Guideline for Structural Health Monitoring. *SAMCO Final Technical Report*.
- Furtner, P., & Veit-Egerer, R. (2011). Approach for the Life Cycle Management of Structures including Durability Analysis, SHM and Maintenance Planning. *Proceedings of the NDTMS 2011 - International Symposium on Nondestructive Testing of Materials and Structures*. Istanbul, Turkey.
- Grimes, C. A., Dickey, E. C., & Pishko, M. V. (2006). *Encyclopedia of Sensors*. American Scientific Publisher .
- H. Wenzel, D. P. (2005). *Ambient Vibration Monitoring*. Chichester Englnd: J. Wiley and Sons Ltd, ISBN 0470024305.
- Jacob, D. L., & Calderone, D. I. (kein Datum). *Nickel Sulphide Inclusions*.
- KEO Int., C. (., & W. A. (2009). *As built drawings - Tower and Facade Elements*.
- Kinematics. (2014). www.kinematics.com.
- KISTLER. (2004). <http://www.kistler.com>. abgerufen am 01.2012.
- Köppl, C. (Mai 2009). *Einflusslinien und ihre Anwendung*. Bachelorarbeit , TU Graz.
- P. Furtner, M. S. (2013). SHM DATA - Management, Treatment, Analysis and Interpretation - a solution for Permanent Monitoring Systems. *Proceedings of the 11th International Conference on Structural Safety & Reliability (ICCOSSAR 2013)*. New York.
- Petersen, D.-I. C. (1980). *Statik und Stabilität der Baukonstruktionen*. Germany : Friedr. Vieweg & Sohn Verlagsgesellschaft GmbH. .
- Swain, M. V. (1981). Nickel sulphide inclusions in glass: an example of microcracking induced by a volumetric expanding phase change. *Journal of Materials Science*, S. 16(1), 151-158.

- VCE. (2015). *www.brimos.at*. Abgerufen am 2015
- VCE ZT GmbH. (2014). *www.vce.at*.
- VCE ZT-GmbH. (2005). *DyGeS*. Wien.
- Veit-Egerer, R., Widmann, M., & Furtner, P. (2011). Structural Assessment of a fire damaged highway bridge in Lagos Nigeria with BRIMOS Structural Health Monitoring . *Proceedings of the 4th International Conference - Experimental Vibration Analysis for Civil Engineering Structures (EVACES 2011)*. Varenna, Italy .
- Wenzel, H. (2009). *Health Monitoring of Bridges*. Chichester England: J. Wiley and Sons Ltd, ISBN 0470031735.
- Wenzel, H., & Egerer, R. V. (18. March 2009). Measurement based traffic loading assessment of steel bridges - a basis for performance prediction. *Structure and Infrastructure Engineering - Maintenance, Management and Life Cycle Design & Performance* .
- Wenzel, H., Veit-Egerer, R., & Widmann, M. (2011). Life Cycle Analysis addressing Maintenance and Repair Options and its affections on Remaining Lifetime. *Proceedings of the ACI Convention Fall 2011 - Bridge Theory and Practice*. Cincinnati, OH, USA.
- Wenzel, H., Veit-Egerer, R., & Widmann, M. (2011). Risk based Civil SHM and life cycle management , SHM and Maintenance Planning . *Proceedings of the 8th International Workshop on Structural Health Monitoring (8th IWSHM)*. Stanford, USA.
- www.wunderground.com*. (kein Datum). Abgerufen am 2013
- Znidaric, A. (2010). *Bridge-WIM as an efficient tool for optimised bridge assesment*. Rom: Frascati ENSA Research Centre.

List of Figures

Figure 1: 35th floor plan of the building (KEO Int. & WS, 2009)	4
Figure 2: Ground floor plan of the building (KEO Int. & WS, 2009)	4
Figure 3: Photo documentation of the tower - overview	5
Figure 4: Photo documentation of the Tower – 37 th floor	5
Figure 5: Overview of the model.....	6
Figure 6: Crossection of the model	6
Figure 7: Beam 44 element specifics (ANSYS, 2012).....	7
Figure 8: SHELL 63 element specifics (ANSYS, 2012)	8
Figure 9: Connection between slab and coloumn.....	8
Figure 10: Foundation.....	9
Figure 11: COBIN14 element specifics (ANSYS, 2012).....	9
Figure 12: MASS21 element specifics (ANSYS, 2012).....	10
Figure 13: BRIMOS nomenclature of dynamic-response-characteristic....	11
Figure 14: 1st mode shape at 0,27 Hz (numerical simulation) – 1st bending mode along transversal axis	12
Figure 15: 2 nd mode shape 0,39 Hz (numerical simulation) – 1 st bending mode along longitudinal axis	12
Figure 16: 3 rd mode shape – 0,67 Hz (numeric simulation) – 1 st torsional mode.....	13
Figure 17: 4 th mode shape – 1,23 Hz (numerical simulation) – 2 nd bending mode along transversal axis	13
Figure 18: 5 th mode shape – 1,65 Hz (numerical simulation) - 2 nd bending mode along longitudinal axis.....	14
Figure 19: 6 th mode shape – 1,72 Hz (numerical simulation) – 2 nd torsional mode.....	14

Figure 20: 7 th mode shape – 2,76 Hz (numerical simulation) – 3 rd bending mode along transversal axis	15
Figure 21: 7 th mode shape – 3,28 Hz (numerical simulation) – 3 rd bending mode along longitudinal axis	15
Figure 22: 3D view of the model	16
Figure 23: 1st mode shape (numerical simulation) – 1st bending around the local transversal axis	18
Figure 24: 2nd mode shape (numerical simulation) – 2nd bending around the local transversal axis	18
Figure 25: 4th mode shape (numerical simulation) – 2nd bending around the local transversal axis	19
Figure 26: 2nd mode shape (numerical simulation) – 2 nd bending around longitudinal axis.....	20
Figure 27: EPI sensor, original housing (TOP), as used (Bottom)	22
Figure 28: Flow chart of BRIMOS Wireless system (VCE, 2015)	23
Figure 29: BRIMOS Wireless unit 1.0 plus EPI sensor example picture (left); picture taken in the gold tower (right)	24
Figure 30: Sensor layout transversal movement (left): expected mode shapes. a = first Eigen frequency b = second c = third; (middle): 2d sensor layout view southwest elevation; (right): 2d sensor layout view southeast elevation	25
Figure 31: 35th floor plan sensor locations	26
Figure 32: Wilcoxon Model 731-207 (right); Mounting of sensor on glass surface inside and outside (left).....	27
Figure 33: Example layout of glass panel with mode shapes (1 st , 2 nd , 3 rd , 4 th)	28
Figure 34: Sensor layout glass panel (right); position of the reference sensor (left)	28
Figure 35: All sensor positions.....	29

Figure 36: example sensor layout with sensor positions (SnP.) and mode shapes (1, 2, 3, 4 and 5).....	31
Figure 37: example of a sensor layout with Line-ups, sensor positions (SnP.) and mode shapes (1, 2, 3, 4, and 5).....	32
Figure 38: Measured glass element at ground floor	33
Figure 39: Measured glass element at 35th floor	34
Figure 40: Measurement signal.....	35
Figure 41: Spectral analysis (ANPSD) for all measurement files, longitudinal direction; 0.3-10 Hz (left) and 0.3 – 4 Hz (right).....	37
Figure 42: Spectral analysis (ANPSD) for all measurement files, transversal direction; 0.1-10 Hz (left) and 0.1 – 6 Hz (right)	38
Figure 43: 1st bending mode – 0,26 Hz, 1BT along transversal axis.....	40
Figure 44: 2nd bending mode – 0,41 Hz, 1BT along longitudinal axis	40
Figure 45: 3rd bending mode – 1,06 Hz, 2BT along transversal axis	41
Figure 46: 2nd torsional mode – 1,41 Hz, 2TL.....	41
Figure 47: 6th bending mode – 2,34 Hz, 3BT along transversal axis	42
Figure 48: 6th bending mode – 2,93 Hz, 3BT along longitudinal axis.....	42
Figure 49: Vibration intensity longitudinal – all points of measurement .	43
Figure 50: Vibration intensity transversal – all points of measurement ..	44
Figure 51: Trend card.....	44
Figure 52: Trend of stiffness distributed over time (entire measurement period), 0,3-6 Hz, longitudinal	45
Figure 53: Trend of stiffness distributed over time (entire measurement period), 0,1-6 Hz, transversal	46
Figure 54: Acceleration signal, all measured channels, façade element 37 th floor	47
Figure 55: Spectral analysis (ANPSD) for all measurement files (in-depth measurement), out-of-plane; 2-100 Hz (left) and 20 – 45 Hz (right) – Panel 2 (37th floor) exemplarily	48

Figure 56: 1st bending mode Panel 2 at 37th floor – 21,94 Hz, 1BT	49
Figure 57: 2nd bending mode Panel 2 at 37th floor – 40,04 Hz, 2BT	49
Figure 58: Boundary conditions used for calculation (Petersen, 1980).....	52
Figure 59: description of ψ (Petersen, 1980).....	53
Figure 60: Buckling value k (Petersen, 1980)	54
Figure 61: Chronological and spatial distribution of broken glass façade elements.....	56
Figure 62: Distribution of broken glass façade elements (top) compared to meteorological data (temperature (middle) and wind speed (bottom))	57

List of Tables

Table 1: Relevant eigenfrequencies	11
Table 2: Relevant eigenfrequencies – single glass panel 37th floor	17
Table 3: Relevant eigenfrequencies – single glass panel ground floor	17
Table 4: Natural Frequencies from the measurement at the tower	39
Table 5: Eigenfrequencies from the measurement at the measured glass façade elements	51
Table 6: Comparison of measurement and numerical simulation – Gold Tower	58
Table 7: Comparison of measurement and numerical simulation – glass façade elements	59
Table 8: Continuation of Table 7	60

